Title

Chapter Two Fe–S Clusters and MutY Base Excision Repair Glycosylases: Purification, Kinetics, and DNA Affinity Measurements

Authors

Nuñez, Nicole N
Majumdar, Chandrima
Lay, Kori T
et al.

Publication Date

2018

DOI

10.1016/bs.mie.2017.11.035

Peer reviewed

HHS Public Access

Author manuscript

Methods Enzymol. Author manuscript; available in PMC 2019 January 10.

Published in final edited form as:

Methods Enzymol. 2018 ; 599: 21–68. doi:10.1016/bs.mie.2017.11.035.

Fe-S Clusters and MutY Base Excision Repair Glycosylases: Purification, Kinetics and DNA Affinity Measurements

N.N. Nuñez[*], **C. Majumdar**[*], **K.T. Lay**[*], and **S. S. David**[*,1]

[*]University of California, Davis, at Davis, CA, United States

Abstract

A growing number of iron-sulfur (Fe-S) cluster cofactors have been identified in DNA repair proteins. MutY and its homologs are base excision repair (BER) glycosylases that prevent mutations associated with the common oxidation product of guanine (G), 8-oxo-7,8-dihydroguanine (OG) by catalyzing adenine (A) base excision from inappropriately formed OG:A mispairs. The finding of an $[4Fe\text{-}4S]^{2+}$ cluster cofactor in MutY, Endonuclease III and structurally similar BER enzymes was surprising and initially thought to represent an example of a purely structural role for the cofactor. However, in the two decades subsequent to the initial discovery, purification and *in vitro* analysis of bacterial MutYs and mammalian homologs such as human MUTYH and mouse Mutyh, have demonstrated that proper Fe-S cluster coordination is required for OG:A substrate recognition and adenine excision. In addition, the Fe-S cluster in MutY has been shown to be capable of redox chemistry in the presence of DNA. The work in our laboratory aimed at addressing the importance of the MutY Fe-S cluster has involved a battery of approaches, with the overarching hypothesis that understanding the role(s) of the Fe-S cluster is intimately associated with understanding the biological and chemical properties of MutY and its unique damaged DNA substrate as a whole. In this chapter, we focus on methods of enzyme expression and purification, detailed enzyme kinetics, and DNA affinity assays. The methods described herein have not only been leveraged to provide insight into the roles of the MutY Fe-S cluster, but have also been provided crucial information needed to delineate the impact of inherited variants of the human homolog MUTYH associated with a colorectal cancer syndrome known as MUTYH Associated Polyposis, or MAP. Notably, many MAP associated variants have been found adjacent to the Fe-S cluster further underscoring the intimate relationship between the cofactor, MUTYH mediated DNA repair and disease.

Keywords

Fe-S cluster; DNA Repair; Protein Purification; Enzyme Kinetics; DNA damage; DNA-protein interactions

1. Introduction

One of the earliest DNA repair enzymes to be discovered containing a $[4Fe\text{-}4S]^{2+}$ cluster was the MutY glycosylase, based on its sequence homology to Endonuclease III (Endo III)

[1]Corresponding author: ssdavid@ucdavis.edu.

(Michaels et al., 1990). MutY and Endo III are DNA glycosylases that initiate base excision repair (BER) by hydrolyzing the glycosidic bond of a damaged or mispaired base from the sugar (David and Wiliams, 1998; Michaels et al., 1990). Subsequent action of other BER pathway enzymes provide for resection of the sugar fragment, and replacement with an appropriate undamaged nucleotide (Manlove et al., 2016). MutY was initially discovered through a combination of genetics and biochemistry (Au et al., 1988; Banda et al., 2017); these studies showed that mutations in the *mutY* gene resulted in increased levels of G:C to T:A transversion mutations and identified an activity in cell lysates capable of mediating repair of G:A mismatches back to G:C base pairs (bps). Purification of the protein product from *Escherichia coli* (*E. coli*, or *Ec*) and analysis on mismatch-containing substrates showed that MutY was an adenine glycosylase that removes A from G:A mismatches, allowing for down-stream BER restoration of a G:C base pair (Au et al., 1989). Subsequent work showed that MutY also exhibited *in vitro* activity on OG:A-mismatches, where OG is 8-oxo-7,8-dihydroguanine (Michaels and Miller, 1992; Porello et al., 1998b). In addition, mutation frequency measurements indicated exceptionally high levels of G:C to T:A transversions upon inactivation of the gene for MutY along with the OG glycosylase Fpg (MutM) in *Ec* (Michaels et al., 1992a; Michaels and Miller, 1992; Michaels et al., 1992b; Miller and Michaels, 1996), leading to the suggestion that OG:A bps are the most important biological substrate for MutY (Banda et al., 2017). The importance of prevention of OG-induced mutations in humans is underscored by the correlation between the inheritance of biallelic mutations within the gene encoding the human MutY homolog (MUTYH) and colorectal polyposis and adenonomas (Al-Tassan et al., 2002; David et al., 2007). This correlation provides for a high probability of colorectal cancer and is referred to as MUTYH-Associated Polyposis or MAP (Al-Tassan et al., 2002).

Nearly all MutY homologs, excluding a few distinct bacterial lineages, possess an Fe-S cluster of the $[4Fe\text{-}4S]^{2+}$ cluster subtype with a unique contiguous spacing of the Cys ligands (Cys-X_6-Cys-X_2-Cys-X_5-Cys) (Fig. 1) (Lukianova and David, 2005; Trasvina-Arenas et al., 2016). The Fe-S cluster in Endo III was originally thought to play a purely structural role in these enzymes due to the fact that the known base excision chemistry would not require a redox cofactor, and the Fe-S cluster was observed to be resistant to reduction or oxidation (Lukianova and David, 2005). Early work in our laboratory involving re-folding experiments of MutY performed in the presence or absence of added Fe (II) and sulfide indicated that the cluster is not needed for overall MutY folding or protein thermal stability (Porello et al., 1998a). However, only forms harboring the Fe-S cluster exhibited affinity for substrate DNA and adenine base excision activity. Notably, these studies were done prior to the development of detailed protocols for analyzing MutY active fraction and kinetics of base excision (methods described in section 3). Although enzyme activity in the Fe-S cluster containing refolded forms was detected, this method is not a robust approach for obtaining significant amounts of highly active, cluster-loaded MutY. Subsequent experiments using site-directed mutagenesis (SDM) to individually replace Fe-S cluster Cys ligands of *Ec* MutY with Ser, His, and Ala demonstrated that a fully coordinated cluster is needed for robust levels of overexpression in bacteria (Lukianova et al., 2005; Golinelli et al., 1999). Methods for obtaining cluster-loaded MutY and mammalian homologs such as human MUTYH are also discussed in detail (section 2).

The first crystal structures of Endo III and the N-terminal domain of MutY suggested that though the Fe-S cluster is located remotely from the active site, it would be critical for substrate engagement (Guan et al., 1998; Lee and Verdine, 2009; Luncsford et al., 2010; Woods et al., 2016). Tainer and co-workers reported the first crystal structure of *Ec* MutY that comprised the catalytic N-terminal domain alone, and harbored the adenine base (Guan et al., 1998). Verdine and co-workers reported a subsequent structure of a catalytically inactive variant of the thermophilic MutY homolog, Asp144Asn *Geobacillus stearothermophilus* (*Gs*) MutY, bound to its natural substrate (an OG:A duplex) in what is known as the lesion recognition complex (LRC) (Fromme et al., 2004). Employment of the cleavage resistant substrate analog *arabino*-2'-fluoro-2'-deoxyadenosine (FA) provided a structure with WT *Gs* MutY enzyme, referred to as the fluorinated lesion recognition complex (FLRC) (Lee et al., 2009). Notably, both the LRC and FLRC structures utilized disulfide cross-linking between the protein and DNA, presumably to stabilize the complex and facilitate crystallization. More recently, we reported the structure of *Gs* MutY bound to an azaribose based transition state (TS) analog-containing duplex which we refer to as the transition state analog complex (TSAC) (Woods et al., 2016) (Fig. 2a). In this case, disulfide crosslinking was not used, and was presumably not required due to the high affinity of *Gs* MutY for the TS mimic duplex.

The TSAC structure, along with kinetics experiments, resulted in a revised S_N1-mechanism for MutY-catalyzed base excision (Fig. 2b) (Woods et al., 2016). Though the reaction catalyzed by MutY appears deceptively simple on paper, MutY must locate rare OG:A bps within the context of the DNA polymer in cells containing a vast excess of structurally similar T:A bps; on average, one OG is present per 10^6–10^7 G bases, with only a fraction of those being OG:A bps. In addition, the adenine base excision process mediated by MutY produces toxic abasic sites opposite the damaged base, OG. Due to the potential for causing single strand breaks, the abasic site product is potentially more detrimental to cells than the initial damaged and mismatched OG:A bp. These complexities require that the process of MutY/MUTYH-mediated base excision be carefully orchestrated with downstream BER enzymes and other DNA-dependent processes in cells.

A conspicuous feature of the MutY structures is a solvent exposed loop, referred to as the Fe-S cluster loop (FCL) motif, that consists of positively charged residues positioned in between two of the Cys residues that coordinate the Fe-S cluster (Guan et al., 1998). The FCL motif is positioned for interactions with the phosphodiester backbone of DNA, and appears to be stabilizing the bent DNA conformation of the bound substrate DNA (Bruner et al., 2000; Fromme et al., 2004). Indeed, key DNA interactions occur via positively charged amino acids within the FCL motif (Brinkmeyer and David, 2015; Chepanoske et al., 2000; Guan et al., 1998). Binding analyses (methods described in section 4) on mutated forms of *Ec* MutY, where the positively charged residues were replaced with alanine, illustrated the importance of these positively charged residues in mediating high affinity for the damaged DNA substrate. Many MAP variants are noted to be positioned in regions localized near the critically bound Fe-S cluster and the FCL (Manlove et al., 2016). For example, MAP variant Pro281Leu is located in the FCL, and this mutation dramatically hampers substrate DNA recognition and adenine excision (Brinkmeyer and David, 2015).

In the process of studying MAP variants localized in the interdomain connector (IDC) region of MUTYH that connects the catalytic N-terminal domain with the C-terminal OG recognition domain, we noticed the presence of three highly conserved Cys residues (Cys-X_6-Cys-X_2-Cys) with spacing surprisingly similar to the Cys spacing of the N-terminal Fe-S cluster (Engstrom et al., 2014). This region of the IDC is not present in bacterial homologs and appears disordered in the N-terminal fragment crystal structure of human MUTYH whose sequence ends abruptly just after these Cys residues (Luncsford et al., 2010). This led us to suspect the presence of an additional metal site due the potential for these residues to serve as an appropriate ligand type and spacing for metal chelation. Metal analysis of *Mus musculus* (*Mm*) Mutyh showed the presence of one zinc ion per four iron atoms (from the N-terminal Fe-S cluster). Site-directed mutagenesis of the proposed Cys ligands resulted in diminished levels of Zn^{2+}, but also demonstrated poor Fe-S cluster loading. Moreover, low levels of Zn^{2+} within the IDC correlated with low levels of active enzyme and ability to suppress DNA mutations. This led us to dub this region as the "Zn^{2+} linchpin motif" to convey its role in properly engaging the OG-binding and catalytic domains on the OG:A mismatch to facilitate adenine base excision (Engstrom et al., 2014).

The role of the FCL and the region around the Fe-S cluster, in mediating DNA binding, suggested that the redox properties of the cluster might be influenced by the presence of DNA. Electrochemical experiments using DNA-modified electrodes have shown that the Fe-S cluster in *Ec* MutY is able to redox cycle with a midpoint potential of +90 mV versus NHE, similar to that observed for high potential (HIPIP) Fe-S cluster proteins (Boon et al., 2003). More recent work using thin film voltammetry on pyrolytic graphite edge electrodes allowed for measurements of both free and bound MutY, and showed a large negative shift in redox potential upon binding to DNA (Bartels et al., 2017). This is consistent with the idea that DNA stabilizes the oxidized form of the cluster, and MutY is a high-potential Fe-S protein (HIPIP) (Ha et al., 2017). In addition, studies of MutY, Endo III and a thermophilic uracil-DNA glycosylase (*Archaeoglobus fulgidus* UDG) have revealed similar potentials for these BER enzymes, and that the electrochemical signal is attenuated if the DNA contains an abasic site or a mismatch (Boal et al., 2005). These studies have led to an intriguing hypothesis that DNA-mediated charge transport (DCT) between Fe-S cluster proteins may aid in the location of DNA damage by sensing the integrity of the DNA helix between two distally located Fe-S cluster containing repair enzymes (Boal et al., 2009; Boal et al., 2007). These ideas are supported by additional studies with Fe-S cluster-containing enzymes participating in DNA repair and replication, such as DNA primase (O'Brien et al., 2017).

Delineating the importance of the MutY Fe-S cluster has relied on a variety of enzyme expression and purification procedures, detailed enzyme kinetics, and DNA binding affinity measurements. In addition, these same strategies were pivotal in establishing the connection between reduced repair of OG:A mismatches due to inheritance of specific MUTYH variants and colorectal cancer (i.e. MAP). This chapter describes protocols that we have developed to study MutY enzymes. We also include examples of how these approaches were used in revealing important features of MutY. Of note, electrochemical approaches used to study MutY, and other Fe-S cluster containing repair and replication proteins, has recently been reported in Methods in Enzymology (Barton et al., 2017). In addition, the chapter following this one (in this volume) focuses on cellular assays used to study MutY enzymes.

Since its inception, our laboratory has been focused on bacterial and mammalian MutY glycosylases and the potential role(s) for the Fe-S cluster with the over-arching hypothesis that revealing the role(s) of the Fe-S cluster cofactor are intimately related to understanding the chemical properties of MutY and MUTYH, as well as deciphering their complex biological functions.

2. Over Expression and Purification of MutY Homologs

2.1 Considerations for Isolating MutY Homologs

The production of Fe-S cluster proteins for *in vitro* analyses can be particularly difficult and warrants thorough consideration of the chosen gene, expression conditions, and subsequent purification scheme. Most biochemical studies to date have used *Ec* MutY, however the thermophilic bacterial homolog *Gs* MutY facilitates X-ray crystallography studies bound to DNA, presumably due to its higher stability (Woods et al., 2016; Wang et al., 2017; Wang et al., 2015; Lee and Verdine, 2009; Fromme et al., 2004). The mammalian homologs (i.e. MUTYH) have high homology to their bacterial cousins, and therefore the bacterial protein can often be a useful surrogate for the human protein. Indeed, the defective activity of MAP variants was initially inferred by the kinetic analysis of the corresponding variants in the *Ec* MutY (Al-Tassan et al., 2002; Banda et al., 2017). However, some regions and positions of MAP-associated variants are only found in the mammalian enzymes requiring use of the mammalian protein (Brinkmeyer and David, 2015; Kundu et al., 2010; Kundu et al., 2009). Levels of overexpression are generally higher using the *Mm* Mutyh compared to *Hs* MUTYH. Depending on the type of experiment to be performed with the metalloprotein, specific considerations will be needed to ensure for accurate enzyme characterization. For example, X-ray absorption spectroscopy fine structure (EXAFS) experiments required the use of a truncated form of *Mm* Mutyh in order to obtain the high concentrations necessary for the study (Engstrom et al., 2014).

Use of an affinity tag in production of Fe-S proteins may aid in overexpression and purification. For example, the use of an N-terminal Maltose Binding Protein (MBP) tag for MutY resulted in significantly higher yields of soluble protein (Boon et al., 2003; Ha et al., 2017). As is the case with MutY, additional constructs such as the *pRKISC* plasmid composed of Fe-S cluster assembly proteins that aid in cellular cluster assembly may be deemed necessary (Tokumoto and Takahashi, 2001). There are commercial sources of MutY (MyBioSource), however, our laboratory's experience is that MutY enzymes are highly sensitive to the storage conditions and do not tolerate repeated freeze thaw cycles. These considerations prompt us to suggest that the commercial enzyme only be used for qualitative applications.

During purification of Fe-S cluster containing enzymes, consideration of the type of environment, such as aerobic versus anaerobic conditions, the presence of reducing agents, degassed buffers, and length of time following cell rupture may influence the quality of protein produced (Crack et al., 2014; Py and Barras, 2010). In addition, supplementation of various media components may also be needed for improved cluster assembly. It is important to bear in mind that perturbations to the Fe-S cluster via introduced amino acid substitutions, especially of the Cys ligands, may result in low yields of protein, resulting in

difficult protein characterization (Engstrom et al., 2014; Golinelli et al., 1999). This section describes the methods rendered necessary for the overexpression and purification of holo MutY and associated Fe-S cluster variants utilizing three model organism homologs.

2.2 Bacteria as an Over Expression Host

Bacterial overexpression of proteins has the advantage of the ease of growth of bacteria and subsequent purification; however, these hosts lack the ability to facilitate post-translational modifications, and may not have optimal codon usage (Kundu et al., 2009). These general procedures were followed for the bacterial host expression of both prokaryotic and mammalian homologs of MutY. In all cases, after the gene is confirmed through sequencing, the cell line (Table 1) is transformed, either through heat shock or through electroporation, with the appropriate expression vector. Transformed cells are then streaked onto LB agar plates with appropriate antibiotic selection (Table 1) and incubated at 37 °C overnight.

The next day, a single colony is selected, and used to inoculate LB starter media (Table 1) which is incubated overnight at 37 °C and 220 rpm in a shaker (Table 3). The following morning, 50 ml of LB starter media is added to 2 L of LB growth media in a 6 L flask that has the same final media components as the starter media. Each flask is incubated at 37 °C and 150 rpm until an optimal OD_{600nm} is reached for induction (Table 1). This is followed by a reduction in temperature to 30 °C, and induction of overexpression by adding IPTG and supplementing with an Fe (II) source (Table 1). After the overexpression period, growth media is centrifuged at 7,500 rpm for 15 min at 4 °C, and, following decanting of the broth, the pellet is suspended in resuspension buffer (Table 1) and stored at −80 °C. Pelleted cells are thawed in an incubator at 37 °C and 150 rpm for 30 min prior to being sonicated on ice for 6 min in 30 s cycles at 70% power (Table 3). The lysate is centrifuged at 12,000 rpm for 15 min, at 4 °C (Table 3). All the steps following this should be carried out at 4 °C and all buffers used should be pre-chilled. The supernatant is decanted into a centrifuge tube on ice, and, if desired, the pellet can be re-suspended and undergo a repeat of sonification and centrifugation.

Troubleshooting tips: Due to the presence of the Fe-S cluster in MutY and homologs, it's important to use reductants when applicable, such as 1 m*M* DTT. Keep in mind that reductants may not be suitable for certain types of affinity tag separation procedures or tag cleavage enzyme incubations. See manufacturer instructions for appropriate reductant concentrations for the type of affinity tag and tag cleavage enzyme being used.

2.3 Purification of *Escherichia coli* MutY

Cloning of the *mutY* gene allowed for sequencing and placement into DNA plasmids for various purposes (Michaels et al., 1990). The first expression plasmid used for MutY was pKKYEco that contained the *mutY* gene under the control on an IPTG inducible promotor (Porello et al., 1996), and this plasmid has been provided to many research groups (Manuel et al., 1996). Much of the biochemical information on MutY has been generated using this un-tagged *Ec* version of the protein. *Ec* MutYΔ226–350 (lacking the C-terminal domain) has been used for structural studies (Guan et al., 1998) and studies that revealed the OG-recognition role of the C-terminal domain (Chmiel et al., 2001). In another example, the X-

ray structure of Cys199His MutYΔ226–350 demonstrated that the His199 side chain was coordinated to the Fe-S cluster, however, there was a reduction in iron occupancy at the site of His coordination giving rise to a larger amount of $[3Fe4S]^{1+}$ cluster (Messick, et al., 2002).

The purification of MutY relies on the combination of several biochemical separation methods, including the precipitation of host cell DNA with streptomycin sulfate following cell lysis, and protein precipitation using ammonium sulfate. This step is followed by desalting and anion exchange columns, and final polishing with a Hi-Trap heparin column (Chmiel et al., 2001; Porello et al., 1996). The details regarding the purification of the *Ec* MutY homolog are detailed in this section.

Once the cells expressing the protein of interest have been lysed via sonication (Table 3), the supernatant is transferred to a sterile beaker, or centrifuge bottle, and enough 25% (w/v) solution of streptomycin sulfate is added to a final concentration of 19%. The solution is stirred for 40 min at 4 °C, and then centrifuged (Table 3) at 5,000 rpm for 10 min to precipitate and pellet out nucleic acids. The supernatant, which appears yellow and viscous, is then decanted into a fresh, sterile beaker or centrifuge bottle, and solid ammonium sulfate is slowly added until its concentration is 40% (w/v). The solution is stirred again for 1 h, to precipitate out the proteins, and then centrifuged at 8,000 rpm for 1 h. The watery supernatant hence obtained is discarded, and the pellet is resuspended in heparin buffer A (Table 2), and filtered sequentially though a 1 μm and then a 0.45 μm filter prior to running on the FPLC (Table 3).

The preceding precipitation steps lead to a high salt concentration of the crude enzyme, and therefore necessitate the use of a desalting column (HiPrep 26/10 Desalting, GE Healthcare). After equilibration of the column with 5 column volumes of buffer, the protein is eluted through an isocratic flow of Heparin Buffer A (Table 2), and fraction collection is cut off at a conductivity of 15–20 mS/cm^2. These fractions are then pooled together, immediately followed by a cation exchange column that is used to separate negatively charged and neutral proteins and residual nucleic acids. This type of separation is possible since the theoretical pI of MutY is 8.3, allowing it to remain positively charged at the pH of the buffers used in this protocol. We use a HiTrap SP HP (Cation) (GE Healthcare) column with a linear gradient of 10–70% Heparin Buffer B (Table 2) to elute the protein.

The eluted fractions are then combined and diluted five-fold with Heparin Buffer A, filtered with a 0.2 μm filter and added to a 5 ml Pharmacia Hi-trap heparin column. MutY is eluted using a linear gradient of 100% Heparin Buffer A to 100% Heparin Buffer B over 20 column volumes (Table 2). Fractions corresponding to MutY can be identified by the signature absorbances measured at 280 nm and 410 nm indicative a protein bearing an Fe-S cluster (Fig. 3). Pure MutY fractions are pooled and diluted in Heparin Buffer A. The sample is then concentrated to the mid μM range (Table 3), and an equal volume of 50% glycerol is added to it, before storing at −80 °C or in liquid nitrogen.

Troubleshooting tips: Prior to use of the cation exchange column, it is important to ensure that the pH of the buffers being used is 7.5, as the MutY will not bind to the column if it is

not positively charged. It is also important to keep in mind the binding capacity of each of the columns being used and ensure that limit is not exceeded. This might necessitate dividing the protein sample into multiple batches and purifying over several runs.

2.4 Purification of a Thermophilic Homolog, *Geobacillus stearothermophilus* MutY

The *Gs* MutY gene was identified via BLAST search of the genome (Fromme et al., 2004) and the gene was cloned into the *pET28a* expression vector (EMD Biosciences). This construct consists of an N-terminal hexa-His tag, followed by a thrombin protease cleavage site prior to the *Gs* MutY gene. In addition, this construct consists of two changes, Phe347Ser and Lys357Glu, to enhance expression yet still retain enzyme activity (Fromme et al., 2004). The protein is overexpressed in BL21 (DE3) Rosetta 2 cells (Novagen) along with the *pRKISC* plasmid that codes for the Fe-S cluster assembly proteins (Table 1) (Tokumoto and Takahashi, 2001).

Following cell lysis, imidazole and NaCl are added to the supernatant to make a final concentration of 20 m*M* and 300 m*M,* respectively. The supernatant is batch bound to Ni^{2+}-NTA resin (Qiagen) for 1 h, poured over a PD10 column, and allowed to flow through by gravity. Following completion of flow through, the column is washed with 10 ml of separation wash buffer and eluted in 3 ml separation elutant buffer (Table 2) and is then concentrated with stirring (Table 3). The protein is filtered with a 0.2 μm filter then purified on an FPLC (Table 3) with an anion exchange MonoQ column (where the column volume, CV=1 ml) that is pre-equilibrated with MonoQ start buffer (20 m*M* Tris-HCl pH 8.0, 5 m*M* β-mercaptoethanol) running at a flow rate of 0.5 ml/min. The sample is eluted over 20 CV of a linear gradient of 0 to 100 % MonoQ elution buffer (MonoQ start buffer with 1 *M* NaCl). *Gs* MutY should elute at approximately 400 m*M* NaCl, and these fractions are then combined and buffer exchanged into storage buffer (Table 2).

To cleave the His-tag from MutY, the solution is diluted and 2 U thrombin (Novagen) per mg enzyme is added to the solution and incubated for 16–20 h at 4 ºC. The thrombin reaction is subsequently inhibited by adding the protease inhibitor PMSF (final concentration of 1 m*M*) and incubated for 2 h at 4 ºC. To the supernatant, imidazole and NaCl is added to make a final concentration of 20 m*M* and 300 m*M* respectively. The supernatant is again batch bound to fresh Ni^{2+}-NTA resin for 1 h, poured over a PD10 column, washed with an additional 2 ml separation wash buffer, which is added to the flow through containing the cleaved MutY protein.

The protein is then further purified by gel-filtration on a Superdex 200 column (GE Healthcare). Prior to loading on the column, the protein sample is concentrated (Table 3) to approximately 300 μl and filtered through a 0.2 μm spin filter (Table 3). The column is pre-equilibrated with 5 CV of storage buffer (pH 8.0) at a flow rate of 0.5 ml/min, following which the protein sample is loaded onto it. Pure *Gs* MutY fractions are pooled and can be concentrated (Table 3) and buffer exchanged into the appropriate storage buffer (Table 2), and finally mixed with glycerol to 25 % final concentration and stored at −80 ºC for future use.

Troubleshooting tips: Since the final purification step involves gel filtration, it is important to concentrate the protein sample to as small a volume as feasible, while avoiding aggregation. This can be achieved through the use of centrifugal concentration units, with regular mixing in-between concentrations.

2.5 MBP-MutY for Higher Yields and Solubility

Use of a maltose-binding protein (MBP) tag fused to the N-terminus of MutY aids in purification and increases protein solubility. The MBP-MutY construct was created by cloning the *Ec MutY* gene into the *pMAL-c2x* expression vector (NEB). The resulting MBP-MutY protein overexpresses better than the un-tagged enzyme, with the overall yield and quality of protein produced being significantly higher (Boon et al., 2003; Chmiel et al., 2001). The MBP-MutY was useful for obtaining the concentrations needed for the first electrochemistry experiments (Boon et al., 2003), as well as more recent electrochemistry and XAS studies (Bartels et al., 2017; Ha et al., 2017).

Overexpression and growth conditions for expressing MBP-MutY that should be followed are outlined in Table 1, with a key feature of inclusion of glucose in the media. After sonication of cells expressing MBP-MutY, the combined supernatant is batch bound to amylose resin (NEB) for 1 h, poured over a PD10 column allowing flow through to complete, and washed with separation buffer A and eluted in separation buffer B (Table 2) followed by concentrating (Table 3). MBP-MutY is then diluted 10-fold in heparin buffer A (Table 2) to lower the salt concentration and is filtered with a 0.2 μm syringe filter.

Directly following, the sample can be added to a 5 ml Pharmacia Hi-trap heparin column on an FPLC (Table 3), and eluted using a linear gradient in heparin buffer A to 100% heparin buffer B (Table 2) over 20 CV. Fractions corresponding to MBP-MutY can be identified by the absorbance measured at 280 nm (protein) and 410 nm (Fe-S cluster) (Fig. 3). Pure fractions can be combined and concentrated (Table 3) to mid to low μM protein concentrations. The enzyme should be buffer exchanged into MutY storage buffer (Table 2) and concentrated to mid to low μM concentrations, and stored as single use aliquots at −80 °C. Purity of MBP-MutY samples can be confirmed via 12% SDS PAGE stained with SYPRO Ruby stain according to manufacturer's procedure.

2.6 Bacterial Expression of *Mus musculus* Mutyh

Overexpression and purification of human MUTYH is notoriously finicky, producing low yields and quality of protein (Engstrom et al., 2014; Golinelli et al., 1999). However, high sequence homology between human MUTYH and other model organism homologs such as mouse Mutyh, provide alternative routes to overcome the challenges of working with the human enzyme (Parker et al., 2003). An expression vector (*pQE30)* encoding Mutyh lacking 28 N-terminal amino acids (Yang et al., 2001) produces active mouse Mutyh, however the *pQE30* vector does not allow for removal of the hexa-His tag (Pope et al., 2005). To utilize this platform but allow for the ability of tag cleavage, the *Mutyh* gene was removed using restriction digestion, and cloned into a *pET28a* vector (EMD Biosciences) equipped with an N-terminal His_6 tag and thrombin cleavage site to allow for preparation of the untagged Mutyh enzyme (Engstrom et al., 2014).

Following cell lysis steps, imidazole and NaCl are added to the supernatant to make a final concentration of 20 m*M* and 1 *M* respectively. The supernatant is batch bound to Ni^{2+}-NTA resin (Qiagen) for 1 h, poured over a PD10 column allowing flow through to move by gravity. Following completion of flow through, wash with 10 ml Mutyh separation wash buffer and elute in 3 ml Mutyh separation elutant buffer (Table 2).

The protein solution should then be diluted 10-fold with Heparin Buffer A (Table 2) to lower the salt and imidazole concentration. To cleave the His-tag from Mutyh, 2 U thrombin (Novagen) per mg Mutyh is added to the solution and incubated for 16–20 h. Subsequent incubation for 2 h with PMSF (final concentration of 1 m*M*). To the supernatant, imidazole and NaCl is added to make a final concentration of 20 m*M* and 1 *M* respectively. The supernatant is again batch bound to clean Ni^{2+}-NTA resin for 1 h, poured over a PD10 column, and washed with an additional 2 ml Mutyh separation wash buffer, which is added to the flow through containing the cleaved Mutyh protein.

Mutyh should be diluted 10-fold in Heparin Buffer A (Table 2) to lower salt concentration, filtered with a 0.2 μm filter, and added to a 5 ml Pharmacia Hi-trap heparin column on an FPLC (Table 3), and eluted using a linear gradient of 100% Heparin buffer A to 100% Heparin Buffer B over 20 CV. Fractions corresponding to Mutyh can be combined and concentrated (Table 3), to mid to low μM concentrations. The enzyme is buffer exchanged into Mutyh storage buffer (Table 2) and concentrated to mid to low $_{\mu}M$ concentrations and stored as single use aliquots at −80 °C. Purity of Mutyh samples are confirmed via 12% SDS PAGE stained with SYPRO Ruby stain as according to manufacturers procedure.

2.7 Eukaryotic Expression System for Production of *Homo sapiens* MUTYH

Mammalian cells and their respective enzymes are inherently complex, with gene products experiencing an assortment of pre- and post-translation modifications. The Bac-to-Bac Baculovirus Expression System (Invitrogen) employs an insect-cell based expression system that incorporates an improved baculovirus transfection procedure to aid in production of eukaryotic proteins. This expression system was found to be particularly useful in producing active human MUTYH amenable to quantitative kinetic analysis (Kundu et al., 2010). To accomplish this, the *MUTYH* 535 amino acid gene isoform and the *malE* gene that codes for an N-terminal MBP tag was previously cloned into the *MCS II* site in the *pFastBacDual* vector, and Arg codons were optimized for expression in the Bac-to-Bac system (Kundu et al., 2010).

The recombinant bacmid is created via transformation into chemically competent DH10Bac (Invitrogen) cells. Uptake colonies can be screened for the recombinant bacmid by performing a blue-white colony-screening assay followed by sequence analysis of the resultant DNA product to check for proper insertion. The transfection procedure closely follows the Bac-to-Bac kit protocol where 1×10^6 Sf9 cells are added to each well of a 6-well cell growth plate and allowed to attach for 1 h at 25 °C. Two transfection reactions are prepared: one with 2 (low) and one with 6 (high) μl of stock plasmid DNA, each of which is then added to 100 μl of MUTYH culture growth media (Table 1), supplemented with 6 μl of Cellfectin, and incubated for 30 min. The media can be carefully decanted and separated from the attached cells, followed by addition of the transfection mixture along with 800 μl of

additional MUTYH culture growth media. The cells are incubated at 28 °C for 5 h, followed by removal of the current transfection mixture and addition of 2 ml fresh MUTYH culture growth media, and subsequently incubated for 72 h at 28 °C to propagate the virus. Following incubation, the media can be centrifuged at 500 *g* for 5 min to pellet cells and debris.

The supernatants are transferred to centrifuge tubes and stored at 4 °C, and a small aliquot of supernatant should be tested via dot blot assay. This will be in comparison to a standard baculovirus of known high titer to determine the ratio of infectious virus particles to cells (or Multiplicity of Infection, MOI). This dot blot assay only requires 2 μl of the standard and viral MUTYH containing supernatants to be detected via dotting on a nitrocellulose membrane, followed by blocking in 5% milk in PBST for 15 min at 25 °C with shaking. The blot can then be visualized with mouse anti-gp64 antibody as according to standard western blot protocol. To generate enough protein for characterization, 600 ml Sf9 cells exponentially growing at >95% viability are seeded at a concentration of 6×10^5 cells/ml in MUTYH culture growth media and then infected with an empirically determined amount of human WT MUTYH baculovirus where the MOI is approximately 3. Following post infection incubation for 65 h, the cells can be centrifuged at 600*g* for 30 min, followed by suspension in 10 ml separation wash buffer.

The cells are to be lysed using a freeze/thaw method of three cycles at 37 °C alternated with three cycles at −80 °C, each lasting for 5 min. All of the following steps are then carried out at 4 °C or on ice unless otherwise noted, and all buffers used are pre-chilled. The cell lysate should be further sonicated (Table 3) two times for 10 s each with a 10 s rest period in between. After sonication, an 18% PEG solution containing 1 *M* NaCl and 10% glycerol is added dropwise to the cell lysate with continuous stirring for 30 min to precipitate out the genomic DNA. The cell lysate is then centrifuged at 15,000*g* for 30 min to pellet cell debris, and 1 ml amylose resin is added to the supernatant and batch bound for 1 h with end-over-end rotation. The slurry is added to a PD10 column allowing flow through to complete via gravity, and washed with 10 column volumes of separation wash buffer (Table 2). Following completion of the wash, 5 ml of separation elution buffer (Table 2) is added to the column and incubated for 30 min. The eluted fractions are combined and concentrated (Table 3) to low μM concentrations and stored as single use aliquots at −80 °C. Purity of MBP-MUTYH samples are confirmed via 12% SDS PAGE stained with SYPRO Ruby stain as according to manufacture procedure.

3. Gel-based Adenine Glycosylase Assays and Measurements of Kinetic Parameters

3.1 General Setup and Execution of the Glycosylase Assay

A general scheme for the gel-based adenine glycosylase assay is depicted in Fig. 4, where MutY (or homolog) is allowed to react with 30 bp radiolabeled DNA substrate containing a central OG:A mispair (Porello et al., 1998b). The reaction is quenched with base at different time points to sever the AP-site containing DNA (resulting from adenine removal) forming a shorter radiolabeled oligonucleotide (nt) product. The 14 nt radiolabeled fragment derived

from the product is separated from the 30 nt radiolabeled fragment derived from the duplex substrate by electrophoresis in a 15% denaturing polyacrylamide gel and visualized using storage phosphor autoradiography. Plots of product concentration as a function of time are obtained and used to determine the rate constants of the enzymatic reaction.

We were initially prompted to more thoroughly investigate the kinetic behavior of MutY in order to explain conflicting data in the literature as to whether OG:A versus G:A bp duplexes are the preferred substrates (Porello et al., 1998b). Our kinetic analysis provided insight into reasons for the apparent contradictions in the literature; a major issue was the lack of appreciation for the much higher affinity of MutY to its OG:AP (abasic) site product duplex (and long half-life ~3 h) compared to the G:AP site product, and the consequences of this on the analysis of MutY activity. Indeed, the intrinsic rate of adenine excision for MutY with OG:A substrates is faster than G:A substrates when analyzed under single turnover (STO) conditions; however, the faster turnover with G:A substrates than OG:A substrates results in more product formed under multiple turnover (MTO) conditions with G:A substrates after long reaction times, and depending on amount of enzyme used. These features make it important to accurately determine the concentration of *active* MutY when performing kinetic experiments so that the experiments can be performed under the proper conditions (STO or MTO). These features also make measuring Michaelis-Menten parameters k_{cat} and K_m with MutY enzymes impractical due to minimal substrate turnover (especially with OG:A substrates) in a reasonable time-frame. Based on our analysis of MutY kinetic behavior, we have developed a kinetic framework for analyzing the processing of DNA substrates by MutY enzymes that balances rigor and simplicity (Fig. 5). The behavior of MutY enzymes can be characterized into three basic steps: “binding” of MutY to the DNA and OG:A mispair (including base-flipping), *N*-glycosidic bond cleavage (base excision) of the A, and release of the abasic site DNA product (Fromme et al., 2004; McCann and Berti, 2008; Michelson et al., 2012; Porello et al., 1998b; Woods et al., 2016). In terms of “binding” we also consider that this involves at least two phases: an initial association with the DNA and encounter with the target bp, followed by flipping of the A from the helix into the enzyme active site (Fig. 5).

By performing the gel-based adenine glycosylase assay under different conditions (multiple-turnover or single-turnover) specific rate constants can be measured to determine the intrinsic rate of base excision catalysis (k_2) and rate of release of the AP site containing DNA product (k_3) (Porello et al., 1998b). Additionally, this assay can be used to determine the active fraction of MutY in a purified sample relative to the total protein concentration determined by absorbance at A_{280nm}.

3.1.1 Radiolabeling the DNA Substrate—A variety of DNA sequences could be used for these assays, however, we have typically used 30 bp duplexes in order to ensure complete duplex formation at the concentrations used in these assays. Most routine assays of MutY enzymes use duplexes containing a central OG:A bp; however, analysis of substrate analogs has often been useful (Chmiel et al., 2001; Chu et al., 2011a; Manlove et al., 2017). We have also found that catalytic deficiencies in MutY enzymes are more often revealed using the non-optimal G:A substrate (Chepanoske et al., 2004; Chmiel et al., 2003; Pope et al., 2002).

The typical 30 nucleotide long DNA oligomers that we have used have the following sequences:

5′-d(CGA TCA TGG AGC CAC **OG**AG CTC CCG TTA CAG)-3′
(University of Utah Health Science Center Core Facilities, OG phosphoramidite purchased from Glen Research)
5′-d(CTG TAA CGG GAG CT**A** GTG GCT CCA TGA TCG)-3′
(Integrated DNA Technologies, IDT)

These oligonucleotides are HPLC purified and desalted using a Dionex DNAPac PA-100 anion exchange column. Oligonucleotides should be stored dried, and only dissolved in solution for quantitation and subsequent labeling. OG-containing oligonucleotides are particularly susceptible to degradation if stored in solution. The 5' end labeled 30 bp long DNA duplex with a centrally placed OG:A mispair is generated by incubating 2.5 pmol of the A containing strand with 25 μCuries of [γ- ^{32}P] ATP (Perkin-Elmer) in the presence of 10 units of T4 polynucleotide kinase (NEB) and the provided kinase buffer, at 37 °C for 30 min. The reaction is terminated by incubating at 90 °C for 5 min. The labeled product is purified using a G-50 microspin column (GE Healthcare), and then freeze dried in a speed-vac under the low heat setting. The dry oligonucleotide is suspended in 2x annealing buffer (Table 4) and combined with an additional 47.5 pmol of unlabeled A containing strand, followed by 60.0 pmol of complementary OG carrying strand to yield a solution of 5% labeled DNA. The final concentration of DNA duplex is brought to 100 n*M* with MilliQ H_2O and the solution is incubated for 5 min at 90 °C on a dry bath incubator, transferred to a Styrofoam box and allowed to cool slowly to 4 °C for 12–16 h to ensure complete annealing.

3.1.2 Preparation of a Denaturing Polyacrylamide Gel—The 15% acrylamide/bisacrylamide gel mixture is prepared according to the composition in Table 4. Degassing the solution for 30 min removes dissolved oxygen after which the solution can be stored in a dark bottle until further use. The gel sandwich for this assay is prepared in a manner similar to that used for DNA sequencing where polymerization of the gel mixture is induced by addition of catalytic amounts of TEMED and ammonium persulfate and the gel is allowed to set for at least 2 h before use.

3.1.3 General Assay Setup—The steps in the glycosylase reaction are illustrated for an active site titration experiment (Fig. 6a) but are similar for STO experiments. Glycosylase assay reactions are carried out in 100 μl volumes total following enzyme addition to the reaction mix (Table 4). The positive and negative controls (excess enzyme and no enzyme, respectively) can be carried out in as little as 20 μl reaction volumes. While the reaction tubes are allowed to equilibrate at 37 °C, the enzyme stock solution is thawed on ice and diluted using ice-cold MutY/MUTYH dilution buffer (Table 4) to give desired enzyme concentrations, in our case 20 n*M*, 40 n*M* and 60 n*M* solutions. These solutions are mixed well before each subsequent tube transfer. The reaction is started by the addition of 10 μl of the 20 n*M* enzyme solution to the 2 n*M* reaction tube while simultaneously starting the timer. The contents of the tube are mixed by gentle and thorough pipetting, and, at each time

point, 8 μl of the reaction mixture is quenched with 2 μl of 1.0 *M* NaOH, immediately incubated at 90 °C for 5 min, and then placed on ice. This process is repeated for the 4 n*M* and 6 n*M* reactions using the 40 n*M* and 60 n*M* enzyme solutions, respectively. The positive and negative controls are incubated at 37 °C for the hour-long duration of the experiment, after which they are also quenched with NaOH.

Troubleshooting tips: In order to avoid losing enzyme activity, mixing the enzyme must be done slowly with a pipette. It is also important to limit the number of freeze-thaw cycles the enzyme undergoes as this will also result in a reduction of activity. Negative controls should indicate quality of labeled DNA. The positive control lane should show a single band corresponding to complete conversion to product; if not, this usually indicates a problem with the DNA, which can sometimes be remedied by re-annealing the DNA or may require use of a new OG (or A) containing oligonucleotide strand.

3.1.4 Visualization and Quantitation of Results—Prior to loading the samples on the gel (Fig. 6b), 10 μl of formamide loading dye (80% formamide, 0.025% xylene cyanol, 0.025% bromophenol blue) is added to each sample, followed by incubation at 90 °C for 10 min, and immediate cooling on ice. The samples are loaded on the premade gel with both wells filled with 1x TBE and run at 1,200 V for 2 h. The gel is then exposed to a phosphor imager screen for 12–15 h, and then scanned (Table 5). The substrate and product band intensities resulting from storage phosphor autoradiogram are quantitated and the data plotted using and appropriate graphing program (Table 5).

3.1.5 Salt Concentration in Assay buffer—A very important consideration in carrying out these experiments is the type and final concentration of salt present in the reaction mixtures. In our laboratory, the glycosylase assay buffer contains NaCl (Table 4), and its concentration is optimized based on the effects of specific and nonspecific DNA interactions under low (30 m*M*) to high (150 m*M*) salt conditions (Livingston et al., 2005; Raetz et al., 2012). The formation of the DNA-enzyme complex is facilitated through hydrogen bonding and electrostatic interactions between the DNA backbone and the amino acid side chains, and it is possible to modulate the extent of these interactions by altering the salt concentrations. At high salt concentrations, the Na^+ cations compete with the enzyme for phosphate binding sites, resulting in lower non-specific interactions between the enzyme and DNA substrate (Record et al., 1991) allowing for the design of experiments to gauge the contribution of these interactions.

Indeed, when the *Ec* homolog of the MAP variant, Tyr82Cys MutY was tested under low and high salt conditions, it was demonstrated to be sensitive to an increase in NaCl concentration, displaying up to a 25-fold reduction in the rate of adenine removal at 150 m*M* NaCl compared to 30 m*M* NaCl, and a 60-fold reduction compared to WT MutY under the same conditions (Livingston et al., 2005). This salt-concentration sensitivity has also been observed with mouse Mutyh and human MUTYH Tyr165Cys disease variants. Under buffer conditions of physiological salt (150 m*M* NaCl) Tyr165Cys displays no OG:A activity yet at lower salt (100 m*M* NaCl), adenine removal is detected albeit with lower extents of reaction completion (Raetz et al., 2012). Substitution of the DNA intercalating residue Tyr at position 82 with Cys at this position may attenuate the possibility for stabilization of the distorted

DNA through intercalation and force the enzyme to bind through electrostatic interactions and hydrogen bonding. Binding of this kind would be disrupted by high salt conditions, and therefore the enzyme is unable to enter its catalytically competent state at 150 m*M* salt, resulting in lower adenine excision (Livingston et al., 2005). Herein, we describe the glycosylase assay, where we carry out this experiment under low salt (i.e. 30 m*M* final NaCl) conditions.

3.2 Correcting the Enzyme Concentration for the Percent Active Fraction

Active fraction measurements of enzymes are important since proteins overexpressed and purified in the laboratory may be improperly folded or truncated, and thus fractions of the enzyme population are inherently, catalytically incompetent (Fersht, 1999; Porello et al., 1998b). The active fraction of different preparations of the same enzyme can widely vary, and these differences must be considered when determining efficiency of catalysis and substrate binding. For example, initial studies concluded that the MAP variants Tyr165Cys and Gly382Asp are completely devoid of activity due to lack of consideration of active fraction (Wooden et al., 2004). However, due to poor bacterial cell based expression of human MUTYH, the enzyme activity must be corrected for the percent active fraction to isolate specific defects in catalysis (Pope et al., 2005; Kundu et al., 2009). In addition, even WT *Ec* MutY displays some variations in percent active fraction amongst varying protein purification procedures, highlighting the importance of correcting for the percent active fraction. These differences may be further exacerbated when comparing MUTYH variants, such as those indicated in MAP, where the amino acid variation may influence stability, folding and ability to actively engage the DNA substrate.

Under conditions of multiple turnover (MTO), the reactions of MutY enzymes are characterized by biphasic kinetics, in which an exponential “burst” of product, formed by *N*-glycosidic bond cleavage, is followed by a steady-state phase of product formation. This kinetic behavior indicates a slow step after the chemistry step, which, in this case, is the release of the enzyme from the AP site-containing DNA product. A convenient aspect of such kinetic behavior is that it allows us to relate the amplitude of the “burst” phase to the active concentration of the enzyme in an active site titration (AST) experiment (Fersht, 1999; Porello et al., 1998b). This percent active enzyme in a given sample of MutY can only be determined if the concentration of the enzyme is greater than K_d. Eq. 1 displays the change in product formation over time, where k_{obs} is the observed rate constant for the burst and k_{ss} is the slope of the linear phase. A_0 is the amplitude of the “burst”, and is equal to the concentration of active MUTYH. This value is obtained by extrapolating the linear portion of the plot to determine the *y*-intercept.

$$[\mathrm{P}]_t = A_0\{1 - \exp(-k_{obs}t)\} + k_{ss}t \quad (1)$$

Each assay is comprised of three trials using a final enzyme concentration of 2 n*M*, 4 n*M* and 6 n*M* (concentration calculated from the A_{280nm} of the protein stock solution). The reaction is quenched at time points 20 s, 40, 1 s, 3 min, 5 min, 10 min, 20 min, 40 min and 1

h using 2.0 μl of 1 *M* NaOH using a set-up similar to that shown in (Fig. 6a). The data is fitted to Eq. 1 to determine the A_0, k_{obs} and k_{ss}. The active enzyme concentration is based on the percentage of active protein out of the total protein concentration based on the A_{280nm}.

3.3 Determining the Rate of Product Release

The rate of release of the AP site containing DNA product from the MutY active site is denoted as the rate constant k_3 (Porello et al., 1998b). Due to the cytotoxicity of AP sites generated by MutY, enzyme variants that result in perturbations of the rate of product release may disrupt the delicate hand off between the glycosylase and downstream repair enzymes (Kundu et al., 2009). Under MTO conditions, the rate constant k_3 is determined from the slope of the linear portion of the product versus time plots. It is important to perform an active site titration of samples incubated in the reaction buffer for various times spanning the planned MTO to ensure the enzyme does not lose activity over the course of the reaction (Kundu et al., 2009). This ensures that the rate of product turnover is not reflective of a decrease in MutY activity, but a steady change in product formation. The rate constant, k_3, is described by Eq. 2 below (Porello et al., 1998b).

$$k_3 = k_{ss}/A_0 \quad (2)$$

3.4 Assessing the Rate of Glycosidic Bond Cleavage

The intrinsic rate on *N*-glycosidic bond cleavage (k_2) of MutY is most conveniently measured using glycosylase assays performed under single turnover (STO) conditions (Porello et al., 1998b), wherein the concentration of active enzyme is higher than that of the substrate DNA (also [E] > K_d). Using these types of experiments has allowed for delineation of the specific effects of amino acid variations in MutY and changes in the mismatch substrate on base excision. The observed rate of product formation can determined from fitting of the production curve to a single exponential using expression 3 below:

$$[P]_t = A_0\{1 - \exp(-k_{obs}t)\} \quad (3)$$

Assuming enzyme-substrate binding is in rapid equilibrium ($k_{off} >> k_2$), k_{obs} is relate to k_2 by:

$$k_{obs} = [E]_0 k_2/(K_d + [E]_0) \quad (4)$$

Where $[E]_0$ refers to the initial enzyme concentration and K_d is the dissociation constant. Under the conditions of single turnover, and when the concentration of enzyme used is well above K_d, this equation reduces to $k_{obs} = k_2$. Thus, the rate constant obtained by plotting the product concentration as a function of time is a measure of the intrinsic rate of adenine base excision by the enzyme (Porello et al., 1998b). The creation of the 5' end labeled DNA substrate and the preparation of reaction and quench tubes is identical to that discussed in

section 2.2. For this assay, the substrate DNA concentration remains 20 n*M*, whereas the enzyme concentration (corrected for active fraction) is at least two-fold higher than that of the substrate DNA. In case of the mammalian homologs of MutY, it may be necessary to increase the enzyme concentration to as much as five-fold that of the substrate DNA concentration. In order to ensure that conditions have been obtained to allow for the $k_{obs} = k_2$ simplification to be made, several concentrations of enzyme in excess should be tested such that k_{obs} is maximized. The product formation is monitored by using the same 15% PAGE described earlier, and the product concentration is fitted to Eq. 3 using a graphing program to determine the rate of glycosidic bond cleavage.

In the case of enzymatic reactions that have a high k_2, such as in the case of WT *Ec* MutY with an OG:A substrate, the rate of the reaction cannot be accurately estimated using the manual kinetic assay described in section 3.3. In this scenario, an automated rapid quench flow instrument may be employed to measure the extent of product formation at time points as short as 0.1 s. In setting up for this experiment, enzyme and DNA reaction mixtures are prepared in 500 μl reaction volumes under conditions consistent with the manual experiments, with the exception that the enzyme is initially incubated with unlabeled non-specific DNA duplex (the 30 bp duplex described in section 3.1.1 with a centrally located G:C base pair) to stabilize it. Typically, 80 n*M* active enzyme is incubated on ice in MutY dilution buffer (Table 4) containing 25 n*M* non-specific duplex supplemented with NaCl for a final concentration of 30 m*M* salt. This enzyme mixture is added to an equal volume of the 40 n*M* labeled DNA substrate to make the final DNA concentration 20 n*M* and final enzyme concentration 40 n*M*. The reaction mixtures are quenched with 0.5 *M* NaOH at time points 0.2 s, 0.5 s, 1 s, 3 s, 7 s, 10 s, 30 s and 60 s and subsequently incubated at 90 ˚C for 5 min. This is followed by electrophoresis on a 15% denaturing polyacrylamide gel, imaging the gel and fitting the change in product concentration over time to Eq. 3 using a graphing program to determine the rate of glycosidic bond cleavage.

Troubleshooting tips: In order to minimize risk of radioactive contamination while using the rapid quench instrument, tubes used to collect quenched reaction should be covered with parafilm beforehand to avoid splash back during ejection. Using rounded tubes, such as 2 ml SealRite rounded microcentrifuge tubes, reduces the risk of a radioactive spill while loading DNA into the syringe used on the rapid quench by eliminating the need to use a needle. To keep the enzyme cold during the experiment, the syringe containing the enzyme should be surrounded by ice using an ice bucket full of ice to cover the bottom and a glove filled with ice to cover the top.

4. Gel-based Assays for Determining MutY-DNA Affinity

4.1 General Features and Considerations of Gel-based Binding Assays with MutY

Previous investigations by our group regarding the roles of the MutY Fe-S cluster demonstrated the importance of the region containing the Fe-S cluster for specific binding to the OG:A containing DNA substrate, via mutations of the ligands to Fe-S cluster, and residues near the Fe-S or part of the FCL motif (Chepanoske et al., 2000; Chepanoske et al., 2004; Porello et al., 1998a). Electrophoretic mobility shift assays (EMSA) are useful for measuring the equilibrium dissociation constant (K_d) for MutY with various DNA duplexes.

Though other types of binding assays may also be used, the high affinity of MutY for substrate, product, and transition state analogs makes use of the EMSA gel-based assay advantageous due to low concentrations of the DNA duplex that can be used, in comparison to other common DNA binding methods, such as fluorescence anisotropy. In these experiments, use of catalytically dead enzyme or a non-cleavable 2'-deoxyadenosine mimic allows for isolation of substrate binding by preventing catalysis. For example, catalytically inactive Glu37Ser *Ec* MutY has previously been used to study binding interactions with the natural substrate OG:A (Livingston et al., 2005). In order to study mutated MutY enzymes and MAP variants, it is convenient to use a non-cleavable analog of A, such as 2'-fluoro-2'-deoxyadenosine (FA). Measurements of affinity to product analogs can also provide a means to evaluate specific aspects of the MutY mechanism. The AP site product formed by MutY adenine excision can be mimicked via incorporation of a product analog such as tetrahydrofuran (THF) into DNA. This analog lacks the hydroxyl group present in the natural AP site; however, its stability and ability to be incorporated into DNA via solid-phase DNA synthesis makes it an attractive substitute for measuring AP site affinity (Chu, et al. 2011a, Woods, et al. 2016). Implementation of EMSAs for determining the dissociation constant of MutY with various DNA contexts is explained in section 4.2.

Transition state analogs are expected to be tight binding inhibitors of enzymes due to the high affinity enzymes have towards transition states; this suggests that the tighter the binding, the more closely the analog resembles the transition state (Pauling, 1948). Kinetic isotope effect studies on MutY have suggested that the reaction mechanism has two distinct oxocarbenium ion-like transition states (McCann and Berti, 2008). In analogy to related nucleosidases and glycosylases, we have developed transition state analogs that feature pyrrolidine nucleotides (Chu et al., 2011a). An exceedingly useful general transition state mimic for BER glycosylases is (3*R*,4*R*)-(hydroxymethyl)pyrrolidin-3-ol (1N), which has a nitrogen in the corresponding 1'-position in the deoxyribose sugar (Woods, et al. 2016). At physiological pH, the protonated amine in 1N mimics the positive charge build-up in the transition state.

Although a powerful tool, the use of tight binding, transition state analogs can result in difficult evaluation and accurate comparison of the dissociation constant, K_d. This is due to limits of detection of the radiolabeled substrate for measuring subnanomolar dissociation constants, which are dependent on the assumption that [enzyme] >> [substrate]. To overcome these limitations, another perspective on binding between the enzyme and DNA can be gained by measuring k_{off}, the dissociation rate constant of the enzyme-substrate complex resulting in free DNA and MutY. Previous work with WT *Gs* MutY and transition state analog, 1N, base paired across from G indicated a K_d below the detection limit, precluding comparing affinity with Asp144Asn MutY (Chu et al., 2011a). However, k_{off} for WT MutY could be accurately calculated using the off rates assay and it showed a 127-fold increased k_{off} for Asp144Asn compared to WT MutY (Chu, 2011b). This variation of EMSA for determining enzyme affinity for DNA is described in section 4.3.

4.1.1 Radiolabeling the DNA Substrate—MutY/MUTYH enzymes have high affinity for their preferred OG:A substrate, and therefore these assays should be performed using DNA concentrations well below the K_d (at least 10-fold lower, ideally 100-fold).

Typically, 5 pmol of the A (or FA) containing oligonucleotide is 5' end labeled. The radiolabeled strand is annealed to a 20% excess of the complementary OG strand and the final concentration of the mixture is brought to, typically, 5 n*M* by the addition of MilliQ H_2O, although higher concentrations can be used so long as the DNA concentration is 10-fold lower than K_d. Annealing is done by incubating the solution for 5 min at 90 °C on a dry bath incubator, transferring the solution to a Styrofoam box, and slowly cooling to 4 °C for 12–16 h. Note, in considering DNA concentration, we assume that no labeled DNA is lost during the post-labeling procedures, so the DNA concentration is likely an overestimate; however, this ensures that the DNA concentration is kept below both the K_d and the enzyme concentration.

Troubleshooting tips: Due to the low concentrations of DNA used in EMSAs, it is best to use freshly labeled DNA (no more than one week old) in order to facilitate band quantitation via storage phosphor autoradiography.

4.1.2 Preparation of a Nondenaturing Polyacrylamide Gel—A 6% non-denaturing polyacrylamide gel (Table 4) is prepared for pouring in the assembled glass plates (Table 6). Polymerization of the gel mixture is induced by addition of catalytic amounts of TEMED and ammonium persulfate and the gel is allowed to set for at least 1 h. Gels are cooled to 4 °C and pre-run at 120 V for 30 min prior to loading.

4.1.3 Running an EMSA—After running the experiment as described in section 4.2, the nondenaturing polyacrylamide gel is loaded with reaction mixtures in a cold room at 4 °C to prevent gel melting. To ensure efficient penetration of the samples into the gel, the running voltage of the gel is increased to 250 V for 10 min prior to and during loading. After the last sample (negative control) has been loaded, the gel is run at 250 V for an additional 10 min. Following this, the voltage is dropped to 120 V and the gel is run for 1.5 h to 2 h or until the lower band of the dye front is about two-thirds of the way down the gel.

Troubleshooting tips: To minimize temperature variation when working with enzyme, allow all pipette tips, gels, and buffers to cool to 4 °C before running the EMSA. Running the gel at higher voltage after loading minimizes dissociation of complexes before entering gel, but may also result in heating, thus the 10 min time-frame is a guideline, and the voltage can be turned-down once all of the samples have entered the gel. We have found the Methods in Enzymology article by J. Carey an excellent resource for tips on running EMSAs of protein-DNA complexes (Carey, 1991).

4.1.4 Visualization and Quantitation of Results—Once the run is complete, the gel is removed from the glass plates and placed in between blotting paper and cellophane (Bio-Rad). The gel is dried for 2 h using a gel dryer (Table 6). The dried gel is developed for three days on a phosphor imager screen, and the resulting autoradiogram is scanned and quantitated. The percent DNA bound is plotted against log[enzyme] and fitted to a one-site binding isotherm using a graphing program to determine K_d.

4.2 Measurements of MutY-DNA Dissociation Constants

Solutions of varying concentrations of the enzyme are titrated against a labeled DNA duplex and allowed to equilibrate at a specific temperature, following which, native PAGE is employed to separate the DNA–enzyme complex from free DNA substrate (Fig. 7). For a one-site binding model, the K_d of the enzyme-substrate complex is expressed as:

$$K_d = [\text{Enzyme}][\text{DNA}]/[\text{Enzyme}\cdot\text{DNA}] \quad (5)$$

In using EMSAs to determine dissociation constants, a constant low concentration of duplex DNA (in the case of *Ec* MutY, a final DNA concentration of 5 p*M*) is equilibrated with a range of enzyme concentrations to determine the enzyme concentration at which half of the DNA is bound. By visual inspection, the lane having roughly the same intensities of bound and free DNA corresponds roughly to the K_d, however, a more accurate value is obtained by fitting to a one-site binding isotherm. Notably, relating enzyme concentration to K_d is only accurate if the DNA concentration is negligible (at least 10–100 fold lower than the [E]). Thus, the [DNA] should be below the lowest enzyme concentration *and* below the expected K_d. Prior to starting the experiment, a reaction mix with the composition detailed in Table 4 is prepared. For a single experiment, 20 μl of the reaction mix is aliquoted into each of 14 microcentrifuge tubes and allowed to equilibrate at 25 °C. Meanwhile, serial dilutions of the enzyme (based on active concentration) are carried out in MutY/MUTYH dilution buffer (Table 4) to give 13 different concentrations. These concentrations should range from at least tenfold greater than the DNA concentration, up to several concentrations that will provide 100% bound DNA. To initiate the experiment, 20 μl of the highest enzyme concentration is added to 20 μl of DNA solution, mixed gently and then incubated at 25 °C for 30 min. This is repeated for each of the enzyme concentrations as well as the negative control. In our assays, the K_d is reported as the average of at least four separate experiments with enzyme concentrations approaching low μ*M* to reach the maximum concentrations needed for saturated substrate binding.

Troubleshooting tips: If the binding titration curves do not fit well to a one-site binding isotherm, this often indicates that the DNA concentration is too high. Binding curves that plateau below 100% bound often indicate a problem with the DNA duplex. This may be due to incomplete annealing or degraded OG-containing oligonucleotide. In addition, homologs or variants that have a lower affinity for the DNA susbtrate may require the use of DNA concentrations as high as 50–100 p*M* in the reaction mixture.

4.3 Measurement of DNA Dissociation Rate (k_{off})

It can be difficult to measure an accurate K_d between MutY and tight binding substrate, transition state and product analogs due to subnanomolar affinity. In addition, use of subnanomolar concentrations of enzyme prevents the use of the assumption that [enzyme] >> [substrate] and, therefore, the model mentioned in 4.2 for calculating K_d fails. To circumvent this issue, another perspective on binding between the enzyme and DNA can be gained by calculating k_{off}, which allows us to measure the rate of release of the DNA and

MutY from the bound substrate-enzyme complex. This is related to the dissociation constant as shown:

$$K_d = k_{\text{off}}/k_{\text{on}} \quad (6)$$

Through Eq. 6, it can be deduced that a larger k_{off} indicates a larger K_d value, suggesting a looser binding interaction. Similar to using an EMSA for calculating the dissociation constant, solutions of enzyme and DNA duplex are allowed to equilibrate at a specific temperature, followed by running a native PAGE to separate the DNA–enzyme complex from free DNA substrate. What differs between the two experiments is the variable is not the concentration of enzyme but rather the time of incubation of the enzyme with DNA. In this procedure, a constant concentration of radiolabeled duplex DNA is equilibrated with excess enzyme, then excess unlabeled duplex DNA is added and incubated for varying lengths of time (Fig. 8).

To begin the experiment, the radiolabeled DNA (section 4.1.1) is incubated with enough enzyme for 30 min at 25 °C to allow for 100% bound DNA. Following equilibration, a 1000-fold excess of unlabeled DNA is added to the reaction mixture. The unlabeled DNA mixture is prepared following the annealing procedure in section 4.1.1. In the case of MutY, 220 μl of the DNA master mix is made with the appropriate amount of enzyme diluted in MutY/MUTYH dilution buffer (Table 4) and 20 p*M* labeled DNA. This is allowed to equilibrate at 25 °C for 30 min. 20 μl of the solution, after 30 min, is loaded onto a gel, prepared by following 4.1.3, as the negative control. To initiate the experiment, the reaction volume is doubled by the addition of 200 μl of unlabeled duplex DNA to the reaction mixture, resulting in 10 n*M* unlabeled duplex DNA, and mixed gently using a pipette. By adding an excess of unlabeled DNA, it is assumed that any enzyme that releases labeled DNA will then bind to unlabeled DNA. 20 μl aliquots of the reaction mixture are loaded onto the gel at the appropriate time points for up to 1 h. The gel is run and quantitated following the procedures found in Section 4.1.3 and 4.1.4, respectively. In the case of a tight binding interaction, it is expected that the labeled DNA will remain mostly bound to the enzyme, resulting in a faint band of unbound DNA (Fig. 8). Alternatively, a loose binding interaction would produce a darker free DNA band, as more of the labeled DNA will be released. From these results, k_{off} can be calculated using the following equation:

$$[\text{DNA}]/[\text{Enzyme}\cdot\text{DNA}] = \text{span}^{-k_{\text{off}}t} + \text{span}_0^{-(k_{\text{off}})_0 t} + \text{plateau} \quad (7)$$

In Eq. 7, a linear transformation is used in the graphing software (Table 6) with the span equal to intercept/gradient, off rate equal to −1/gradient, and plateau is equal to the percent DNA bound when the slope is zero.

Troubleshooting tips: If the concentration of enzyme is too high, this could lead to a super-shifted band in the gel, making quantification difficult. Reduce the enzyme concentration to address this issue.

5. Application of Methods to Reveal Roles of the Fe-S Cluster Cofactor in MutY Homologs

To study the Fe-S cluster of MutY and homologs *in vitro* requires efficient overexpression and purification of the enzyme followed by assessment of repair activity via glycosylase and binding assays. Bacterial overexpression and purification of *Ec* MutY and Cys to His, Ser and Ala variants demonstrated that cluster coordination is essential for producing viable glycosylases capable of recognizing and excising adenine (Lukianova et al., 2005; Golinelli et al., 1999). The utilization of the thermophilic homolog, *Gs* MutY, has aided in the development of several crystal structures of the protein in complex with DNA (Fromme et al., 2004; Woods et al., 2016). The ability to obtain highly concentrated samples of MBP-MutY allowed for XAS studies on MBP-MutY that provided insight into the influence of solvation and DNA on the Fe-S covalency of the MutY Fe-S cluster and its influence on its redox properties (Ha et al., 2017). Production of mammalian homologs, such as the bacterial expression of mouse Mutyh, resulted in identification of a novel Zn^{2+} linchpin motif in higher eukaryotic MUTYH homologs (Engstrom et al., 2014). An insect cell-based expression of human MUTYH allowed for detailed characterization of the functional consequences of several MAP variants (Kundu et al., 2009) and identification of a functionally relevant phosphorylation site (Kundu et al., 2010).

Following purification, it is important to establish the percent active fraction to account for variances between different protein preparations, which is particularly important with mammalian homologs (Porello et al., 1998b; Brinkmeyer and David, 2015). The amplitude of the burst phase from adenine glycosylase assay under MTO conditions is directly related to the active enzyme concentration, and provides a means to correct for the active fraction of a given aliquot of a purified MutY enzyme stock (Porello et al., 1998b). Analysis of the active fraction can also be useful in determining the functional consequences of an amino acid variation, and may be illuminating in terms of the origin of reduced activity for a given variant. Indeed, since MutY adenine excision activity requires proper engagement of MutY on the OG:A mismatch DNA substrate, a reduced active fraction in a mutated MutY/MUTYH enzyme may be due to its inability to bind to the DNA substrate in a productive manner that leads to catalysis.

Analysis of multiple preparations of two MAP variants Pro281Leu and Arg296ys MUTYH (Fig. 9) indicated that both enzymes have significantly reduced active fractions of 0.1 and 5% relative to the WT enzyme, respectively (Brinkmeyer and David, 2015). This suggested reduced engagement with the DNA substrate; indeed, further analysis showed the Pro281Leu MUTYH was completely unable to bind to the OG:FA substrate analog duplex, while Arg295Cys was able to bind, but with reduced affinity (~10-fold). Notably, in the case of Arg295Cys, using correction for active fraction, the intrinsic rate of adenine glycosylase activity (k_2) was similar to WT, indicating that the mutation reduces the fraction of bound catalytically competent enzyme. In contrast, the reduced engagement of Pro281Leu could not simply be corrected by using higher concentrations of enzyme, and in this case, k_2 could not be determined. The results with Pro281Leu and Arg295Cys illustrate the key importance of the FCL motif in facilitating interactions between the positively charged residues of

MUTYH and the negatively charged DNA (Fig. 9, Table 7) (Brinkmeyer and David, 2015). Of note, similar types of results were obtained in studying the Zn^{2+} linchpin mutants, showing the keen insight that can be gained by this type of careful analysis (Engstrom et al., 2014).

Detailed analysis of the kinetic parameters using the glycosylase assays and K_d measurements via EMSA has also revealed the relative importance of specific residues around the Fe-S cluster in mismatch recognition versus adenine excision (Banda et al., 2017; Lukianova and David, 2005). For example, the impact of replacement of three positively charged amino acids in the FCL of MutY (e.g. Arg194Ala, Lys196Ala and Lys198Ala) was discerned by measuring the kinetic parameters of the adenine glycosylase activity (k_2, k_3) with both OG:A and G:A substrates (Chepanoske et al., 2000). In this case, the G:A substrate was particularly useful in revealing the catalytic defect, and has the advantage of not requiring use of the rapid quench instrument for determination of k_2. Notably, all three variants were shown to have similarly decreased affinity (10-fold) for an OG:FA duplex; however, Lys198Ala was shown to have the most dramatic effect on the glycosylase activity measured under STO conditions, illustrating a direct role of Lys198 in mediating mismatch recognition *and* excision. Indeed, a simple “DNA binding” defect would not be expected to impact k_2 since these experiments are performed under concentrations significantly above K_d. Thus, the reduced k_2 for Lys198Ala indicates that the “binding” interaction of Lys198 with the OG:A substrate is critical for catalysis. Notably, mutation of several Lys residues to Ala near the active site had no effect on the measured k_2, illustrating that, though seemingly far from the active site, the FCL and the region around the Fe-S cluster plays a key role in mediating interactions with the damaged substrate, perhaps by helping to facilitate base-flipping and proper placement of the adenine within the active site.

Similarly, Arg143 in MutY was identified to be close to DNA by photocrosslinking, and along with nearby Arg147 is localized within a highly conserved Arg(Val/Leu)XXArg motif in Fe-S cluster BER glycosylases (Chepanoske et al., 2004). These two Arg residues hydrogen-bond to the Fe-S cluster, and are close to the DNA phosphodiester backbone. Both Arg143Ala and Arg147Ala MutY exhibit reduced OG:FA affinity and reduced catalysis with a G:A substrate. Notably, the MAP variant Arg227Trp has also been shown to have reduced mismatch affinity and glycosylase activity (Bai et al., 2005). Kisker and co-workers also noted that there is an Arg in the nucleotide excision repair enzyme XPD positioned similarly these two Arg residues in MutY suggesting that a similar role of the XPD Fe-S cluster in positioning residues for specific interactions with DNA (Wolski et al., 2008).

Fe-S cluster cofactors provide a wealth of diverse biochemical possibilities within the cell, and their discovery in a variety of DNA binding enzymes has significantly increased since the discovery of the cofactor in MutY and Endo III (Boon et al., 2003; O’Brien et al., 2017). The BER glycosylase MutY and MUTYH have served as notable examples, where the methods described herein aided in illustrating the importance of the highly conserved $[4Fe\text{-}4S]^{2+}$ cluster. The cofactor was demonstrated essential for catalytic domain structural stability and base lesion recognition (Lukianova and David, 2005). In addition to being essential for making intimate contacts with DNA, electrochemistry experiments on purified MutY demonstrated that the Fe-S cluster is also capable of performing redox chemistry well

within cell potential ranges, and participates in DNA-mediated charge transport (DCT) processes (Bartels et al., 2017). The DCT abilities of MutY and other DNA binding enzymes is hypothesized to aid these low copy number proteins in locating DNA damage within a biological timescale. The presence of the Fe-S cluster would help circumvent this issue, by allowing the protein to participate in DCT as a means to coordinate DNA replication and repair. These discoveries build upon the development and implementation of methods described in this chapter and the accompanying chapter in this volume. Indeed, a suite of methods and approaches are needed to reveal the complexity of roles for Fe-S cluster-bearing DNA binding enzymes, such as MutY, in maintaining genomic integrity.

References

Al-Tassan N, Chmiel NH, Maynard J, Fleming N, Livingston AL, Williams GT, Hodges AK, Davies DR, David SS, Sampson JR, and Cheadle JR (2002). Inherited variants of MYH associated with somatic G : C -> T : A mutations in colorectal tumors. Nat Genet 30, 227–232. [PubMed: 11818965]

Au KG, Cabrera M, Miller JH, and Modrich P (1988). Escherichia coli mutY gene product is required for specific A-G----C.G mismatch correction. Proc Natl Acad Sci U S A 85, 9163–9166. [PubMed: 3057502]

Au KG, Clark S, Miller JH, and Modrich P (1989). Escherichia coli mutY gene encodes an adenine glycosylase active on G-A mispairs. Proceedings of the National Academy of Sciences 86, 8877–8881.

Bai H, Jones S, Guan X, Wilson TM, Sampson JR, Cheadle JP, and Lu A-L (2005). Functional characterization of two human MutY homolog (hMYH) missense mutations (R227W and V232F) that lie within the putative hMSH6 binding domain and are associated with hMYH polyposis. Nucleic Acids Res 33, 597–604. [PubMed: 15673720]

Banda DM, Nuñez NN, Burnside MA, Bradshaw KM, and David SS (2017). Repair of 8- oxoG:A mismatches by the MUTYH glycosylase: Mechanism, metals and medicine. Free Radical Biology and Medicine 107, 202–215. [PubMed: 28087410]

Bartels PL, Zhou A, Arnold AR, Nuñez NN, Crespilho FN, David SS, and Barton JK (2017). Electrochemistry of the [4Fe4S] Cluster in Base Excision Repair Proteins: Tuning the Redox Potential with DNA. Langmuir 33, 2523–2530. [PubMed: 28219007]

Barton JK, Bartels PL, Deng Y and O'Brien E (2017). Electrical probes of DNA-binding proteins. Methods in Enzymology 591 355–414. [PubMed: 28645377]

Boal AK, Genereux JC, Sontz PA, Gralnick JA, Newman DK, and Barton JK (2009). Redox signaling between DNA repair proteins for efficient lesion detection. Proceedings of the National Academy of Sciences 106, 15237–15242.

Boal AK, Yavin E, and Barton JK (2007). DNA repair glycosylases with a [4Fe-4S] cluster: a redox cofactor for DNA-mediated charge transport? J Inorg Biochem 101, 1913–1921. [PubMed: 17599416]

Boal AK, Yavin E, Lukianova OA, O'Shea VL, David SS, and Barton JK (2005). DNA-bound redox activity of DNA repair glycosylases containing [4Fe-4S] clusters. Biochemistr y-Us 44, 8397–8407.

Boon EM, Livingston AL, Chmiel NH, David SS, and Barton JK (2003). DNA-mediated charge transport for DNA repair. P Natl Acad Sci USA 100, 12543–12547.

Brinkmeyer MK, and David SS (2015). Distinct functional consequences of MUTYH vari ants associated with colorectal cancer: Damaged DNA affinity, glycosylase activity and interaction with PCNA and Hus1. DNA Repair (Amst) 34, 39–51. [PubMed: 26377631]

Bruner SD, Norman DP, and Verdine GL (2000). Structural basis for recognition and repair of the endogenous mutagen 8-oxoguanine in DNA. Nature 403, 859–866. [PubMed: 10706276]

Carey J (1991). Gel retardation. Methods in Enzymology 208, 103–117. [PubMed: 1779832]

Chepanoske CL, Golinelli MP, Williams SD, and David SS (2000). Positively charged residues within the iron-sulfur cluster loop of E-coli MutY participate in damage recognition and removal. Arch Biochem Biophys 380, 11–19. [PubMed: 10900127]

Chepanoske CL, Lukianova OA, Lombard M, Golinelli-Cohen MP, and David SS (2004). A residue in MutY important for catalysis identified by photocross-linking and mass spectrometr y. Biochemistry-Us 43, 651–662.

Chmiel NH, Golinelli MP, Francis AW, and David SS (2001). Efficient recognition of substrates and substrate analogs by the adenine glycosylase MutY requires the C -terminal domain. Nucleic Acids Res 29, 553–564. [PubMed: 11139626]

Chmiel NH, Livingston AL, and David SS (2003). Insight into the functional consequences of inherited variants of the hMYH adenine glycosylase associated with colorectal cancer: Complementation assays with hMYH variants, and pre-steady-state kinetics of the corresponding mutated E-coli enzymes. J Mol Biol 327, 431–443. [PubMed: 12628248]

Chu AM, Fettinger JC, and David SS (2011a). Profiling base excision repair glycosylases with synthesized transition state analogs. Bioorg Med Chem Lett 21, 4969–4972. [PubMed: 21689934]

Chu AM (2011b). Synthesis and characterization of azaribose transition state analogs of base excision repair glycosylases. Ann Arbor: University of California, Davis Thesis Dissertation.

Crack JC, Green J, Thomson AJ, and Le Brun NE (2014). Techniques for the production, isolation, and analysis of iron-sulfur proteins. Methods in molecular biology 1122, 33–48. [PubMed: 24639252]

David SS, O'Shea VL, and Kundu S (2007). Base-excision repair of oxidative DNA damage. Nature 447, 941–950. [PubMed: 17581577]

David SS, and Wiliams SD (1998). Chemistry of glycosylases and endonucleases involved in base-excision repair. Chem Rev 98, 1221–1261. [PubMed: 11848931]

Engstrom LM, Brinkmeyer MK, Ha Y, Raetz AG, Hedman B, Hodgson KO, Solomon EI, and David SS (2014). A zinc linchpin motif in the MUTYH glycosylase interdomain connector is required for efficient repair of DNA damage. J Am Chem Soc 136, 7829–7832. [PubMed: 24841533]

Fersht A (1999). Structure and mechanism in protein science : a guide to enzyme catalysis and protein folding. In, (New York :: W.H. Freeman).

Fromme JC, Banerjee A, Huang SJ, and Verdine GL (2004). Structural basis for removal of adenine mispaired with 8-oxoguanine by MutY adenine DNA glycosylase. Nature 427, 652–656. [PubMed: 14961129]

Golinelli MP, Chmiel NH, and David SS (1999). Site-directed mutagenesis of the cysteine ligands to the [4Fe-4S] cluster of Escherichia coli MutY. Biochemistry-Us 38, 6997–7007.

Guan Y, Manuel RC, Arvai AS, Parikh SS, Mol CD, Miller JH, Lloyd S, and Tainer JA (1998). MutY catalytic core, mutant and bound adenine structures define specificity for DNA repair enzyme superfamily. Nature structural biology 5, 1058–1064. [PubMed: 9846876]

Ha Y, Arnold AR, Nunez NN, Bartels PL, Zhou A, David SS, Barton JK, Hedman B, Hodgson KO, and Solomon EI (2017). Sulfur K-Edge XAS Studies of the Effect of DNA Binding on the [Fe4S4] Site in EndoIII and MutY. J Am Chem Soc 139, 11434–11442. [PubMed: 28715891]

Kundu S, Brinkmeyer MK, Eigenheer RA, and David SS (2010). Ser 524 is a phosphorylation site in MUTYH and Ser 524 mutations alter 8-oxoguanine (OG): A mismatch recognition. DNA Repair 9, 1026–1037. [PubMed: 20724227]

Kundu S, Brinkmeyer MK, Livingston AL, and David SS (2009). Adenine removal activity and bacterial complementation with the human MutY homologue (MUTYH) and Y165C, G382D, P391L and Q324R variants associated with colorectal cancer. DNA Repair (Amst) 8, 1400–1410. [PubMed: 19836313]

Lee S, and Verdine GL (2009). Atomic substitution reveals the structural basis for substrate adenine recognition and removal by adenine DNA glycosylase. Proceedings of the National Academy of Sciences 106, 18497–18502.

Livingston AL, Kundu S, Pozzi MH, Anderson DW, and David SS (2005). Insight into the roles of tyrosine 82 and glycine 253 in the Escherichia coli adenine glycosylase MutY. Biochemistry-Us 44, 14179–14190.

Lukianova OA, and David SS (2005). A role for iron-sulfur clusters in DNA repair. Curr Opin Chem Biol 9, 145–151. [PubMed: 15811798]

Luncsford PJ, Chang D-Y, Shi G, Bernstein J, Madabushi A, Patterson DN, Lu AL, and Toth EA (2010). A Structural Hinge in Eukaryotic MutY Homologues Mediates Catalytic Activity and Rad9–Rad1–Hus1 Checkpoint Complex Interactions. J Mol Biol 403, 351–370. [PubMed: 20816984]

Manlove AH, McKibbin PL, Doyle EL, Majumdar C, Hamm ML, and David SS (2017). Structure-Activity Relationships Reveal Key Features of 8-Oxoguanine: A Mismatch Detection by the MutY Glycosylase. ACS chemical biology 12, 2335–2344. [PubMed: 28723094]

Manlove AH, Nuñez NN, and David SS (2016). The GO Repair Pathway: OGG1 and MUTYH In The Base Excision Repair Pathway, (WORLD SCIENTIFIC), pp. 63–115.

Manuel RC, Czerwinski EW, and Lloyd RS (1996). Identification of the structural and functional domains of MutY, an Escherichia coli DNA mismatch repair enzyme. J Biol Chem 271, 16218–16226. [PubMed: 8663135]

McCann JAB, and Berti PJ (2008). Transition-State Analysis of the DNA Repair Enzyme MutY. J Am Chem Soc 130, 5789–5797. [PubMed: 18393424]

Michaels ML, Cruz C, Grollman AP, and Miller JH (1992a). Evidence that MutY and MutM combine to prevent mutations by an oxidatively damaged form of guanine in DNA. Proceedings of the National Academy of Sciences 89, 7022–7025.

Michaels ML, and Miller JH (1992). The GO system protects organisms from the mutagenic effect of the spontaneous lesion 8-hydroxyguanine (7,8-dihydro-8-oxoguanine). J Bacteriol 174, 6321–6325. [PubMed: 1328155]

Michaels ML, Pham L, Nghiem Y, Cruz C, and Miller JH (1990). MutY, an adenine glycosylase active on G-A mispairs, has homology to endonuclease III. Nucleic Acids Res 18, 3841–3845. [PubMed: 2197596]

Michaels ML, Tchou J, Grollman AP, and Miller JH (1992b). A repair system for 8-oxo-7,8-dihydrodeoxyguanine. Biochemistry-Us 31, 10964–10968.

Michelson AZ, Rozenberg A, Tian Y, Sun XJ, Davis J, Francis AW, O'Shea VL, Halasyam M, Manlove AH, David SS, and Lee JK (2012). Gas-Phase Studies of Substrates for the DNA Mismatch Repair Enzyme MutY. J Am Chem Soc 134, 19839–19850. [PubMed: 23106240]

Miller JH, and Michaels M (1996). Finding new mutator strains of Escherichia coli--a review. Gene 179, 129–132. [PubMed: 8955638]

O'Brien E, Holt ME, Thompson MK, Salay LE, Ehlinger AC, Chazin WJ, and Barton JK (2017). The [4Fe4S] cluster of human DNA primase functions as a redox switch using DNA charge transport. Science 355.

Pauling L (1948). Nature of forces between large molecules of biological interest. Nature 161, 707–709. [PubMed: 18860270]

Pope MA, Porello SL, and David SS (2002). Escherichia coli apurinic-apyrimidinic endonucleases enhance the turnover of the adenine glycosylase MutY with G : A substrates. J Biol Chem 277, 22605–22615. [PubMed: 11960995]

Porello SL, Cannon MJ, and David SS (1998a). A substrate recognition role for the [4Fe- 4S](2+) cluster of the DNA repair glycosylase MutY. Biochemistry-Us 37, 6465–6475.

Porello SL, Leyes AE, and David SS (1998b). Single-turnover and pre-steady-state kinetics of the reaction of the adenine glycosylase MutY with mismatch-containing DNA substrates. Biochemistry-Us 37, 14756–14764.

Porello SL, Williams SD, Kuhn H, Michaels ML, and David SS (1996). Specific recognition of substrate analogs by the DNA mismatch repair enzyme MutY. J Am Chem Soc 118, 10684–10692.

Py B, and Barras F (2010). Building Fe–S proteins: bacterial strategies. Nat Rev Micro 8, 436–446.

Raetz AG, Xie YL, Kundu S, Brinkmeyer MK, Chang C, and David SS (2012). Cancer- associated variants and a common polymorphism of MUTYH exhibit reduced repair of oxidative DNA damage using a GFP-based assay in mammalian cells. Carcinogenesis 33, 2301–2309. [PubMed: 22926731]

Record MT, Ha J-H, and Fisher MA (1991). [16] Analysis of equilibrium and kinetic measurements to determine thermodynamic origins of stability and specificity and mechanism of formation of site-specific complexes between proteins and helical DNA. Methods in enzymology 208, 291–343. [PubMed: 1779839]

Tokumoto U, and Takahashi Y (2001). Genetic analysis of the isc operon in Escherichia coli involved in the biogenesis of cellular iron-sulfur proteins. Journal of biochemistry 130, 63–71. [PubMed: 11432781]

Trasvina-Arenas CH, Lopez-Castillo LM, Sanchez-Sandoval E, and Brieba LG (2016). Dispensability of the [4Fe-4S] cluster in novel homologues of adenine glycosylase MutY. The FEBS journal 283, 521–540. [PubMed: 26613369]

Wang L, Chakravarthy S, and Verdine GL (2017). Structural Basis for the Lesion-scanning Mechanism of the MutY DNA Glycosylase. J Biol Chem 292, 5007–5017. [PubMed: 28130451]

Wang L, Lee SJ, and Verdine GL (2015). Structural Basis for Avoidance of Promutagenic DNA Repair by MutY Adenine DNA Glycosylase. J Biol Chem 290, 17096–17105. [PubMed: 25995449]

Wolski SC, Kuper J, Hanzelmann P, Truglio JJ, Croteau DL, Van Houten B, and Kisker C (2008). Crystal structure of the FeS cluster-containing nucleotide excision repair helicase XPD. PLoS biology 6, e149. [PubMed: 18578568]

Woods RD, O'Shea VL, Chu A, Cao S, Richards JL, Horvath MP, and David SS (2016). Structure and stereochemistry of the base excision repair glycosylase MutY reveal a mechanism similar to retaining glycosidases. Nucleic Acids Res 44, 801–810. [PubMed: 26673696]

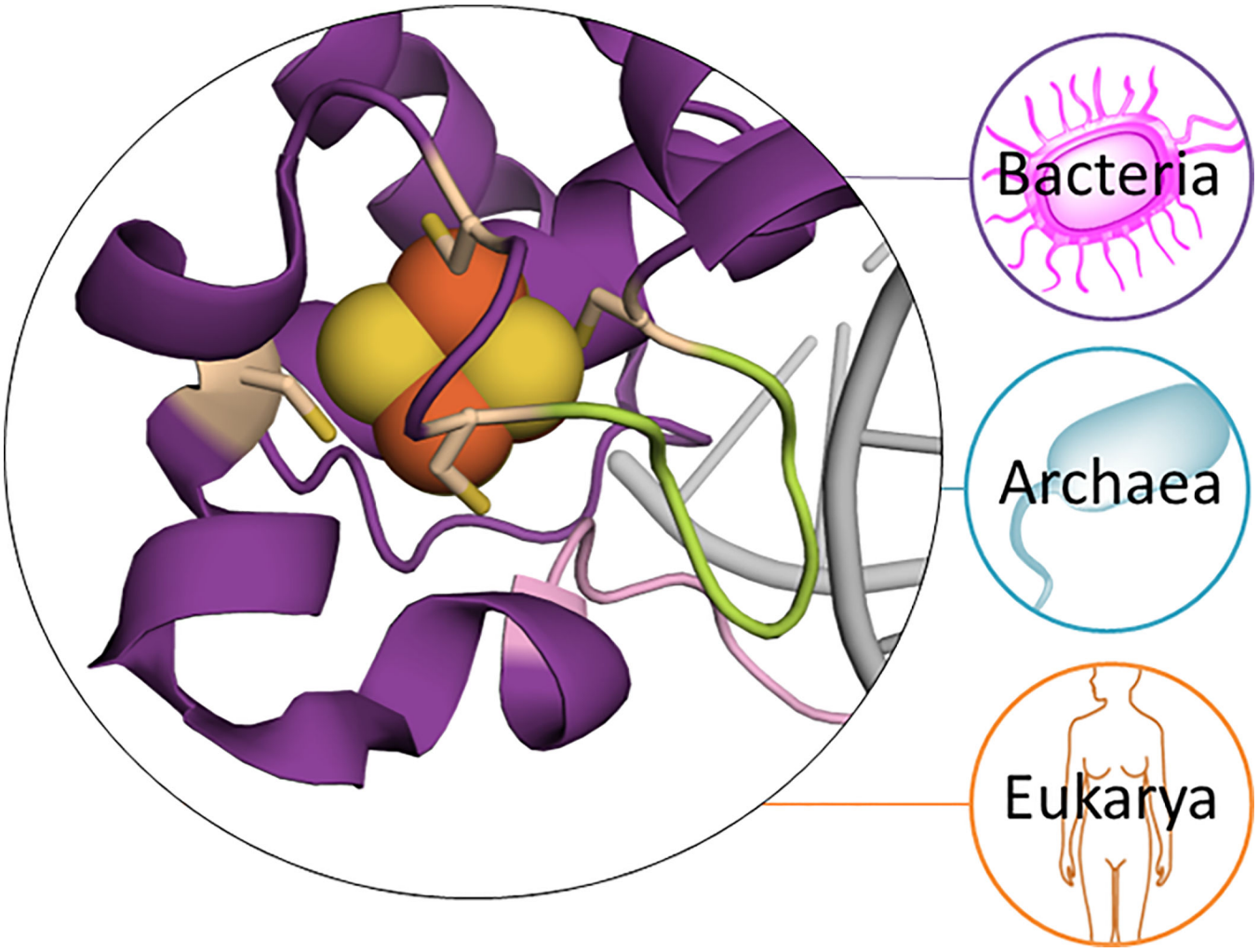

Figure 1. MutY Fe-S Cluster.

As seen in the crystal structure of *Geobacillus stearothermophilus* MutY (PDB 5DPK) (purple) (Woods et al., 2016), the $[4Fe\text{-}4S]^{2+}$ cluster (orange and yellow spheres) is coordinated by four Cys ligands (beige colored sticks), and homolog lineages bearing the iconic Fe-S cluster span throughout all three domains of life. Notably, the Fe-S cluster is important for providing key contacts with the DNA (grey) via positioning of the FCL (green) generated by the first two Cys in the Cys-X_6-Cys-X_2-Cys-X_5-Cys conserved motif, and is located adjacent to the start of the IDC (light pink) (Guan et al., 1998).

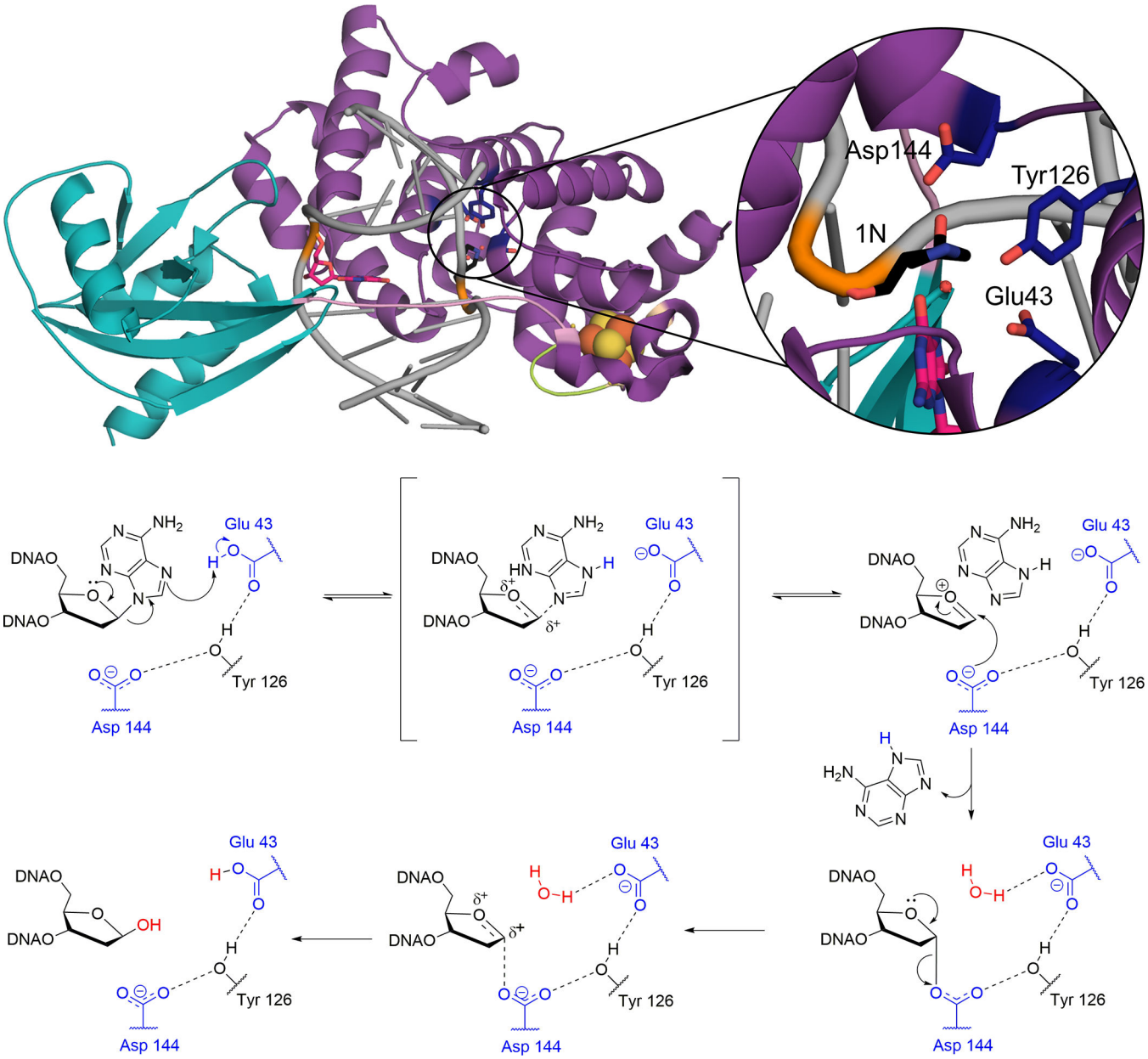

Figure 2. Structure and Updated Mechanism for MutY

a) Crystal structure of *Gs* MutY (PDB ID: 5DPK) bound to DNA (grey) containing OG (hot pink) opposite the pyrrolidine transition state mimic, 1N (black) (Woods et al., 2016). MutY has several structural features, including the N-terminal domain (purple) that houses the Fe-S cluster (orange and yellow spheres) and FCL (green), which is connected to the C-terminal domain (teal), via the IDC (light pink). b) Mechanism of adenine removal by MutY and homologs where active site residues are marked in blue and numbered according to their positions in *Gs* MutY. The adenine base is first protonated by Glu43 to form a good leaving group, and dissociates from the sugar via an S_N1-like mechanism. The resulting oxocarbenium ion is proposed to be stabilized though the formation of a covalent

intermediate with Asp144, which dissociates upon nucleophilic attack by an activated water molecule (red) to form the abasic site product.

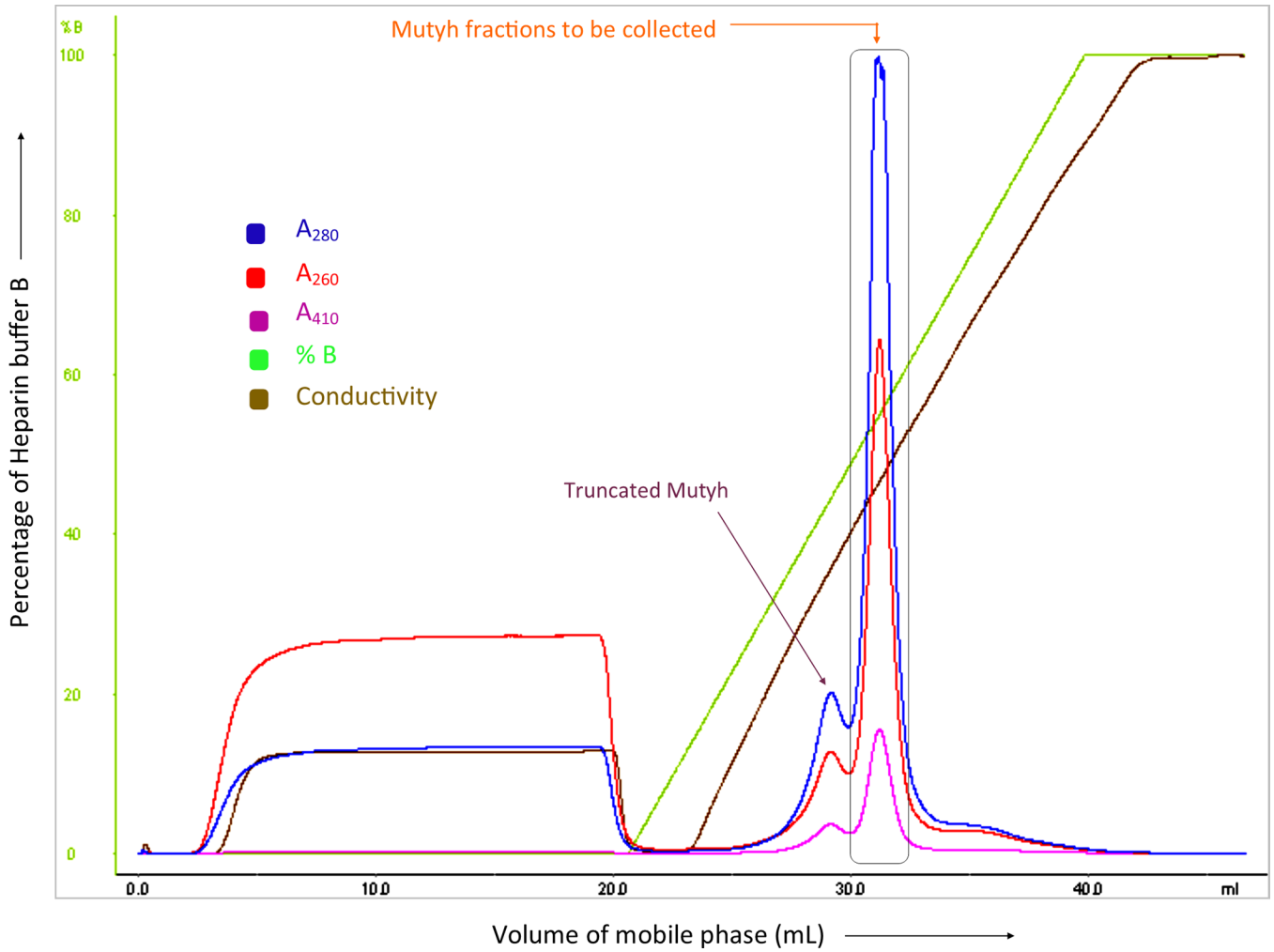

Figure 3. Representative chromatogram of Mutyh during purification through a Hi-Trip Heparin column.

The blue, red and pink lines refer to the absorbance at 280 nm, 260 nm and 410 nm wavelengths, respectively, while the green and brown lines refer to the percentage of heparin buffer B and the conductivity of the sample. Mutyh and its homologs have similar chromatograms, and typically elute at a NaCl concentration of 450 m*M* as shown by the peak above. The peak eluted just prior to the main protein peak is truncated protein and is collected in separate fractions to prevent contamination of the full-length enzyme (Pope et al., 2005).

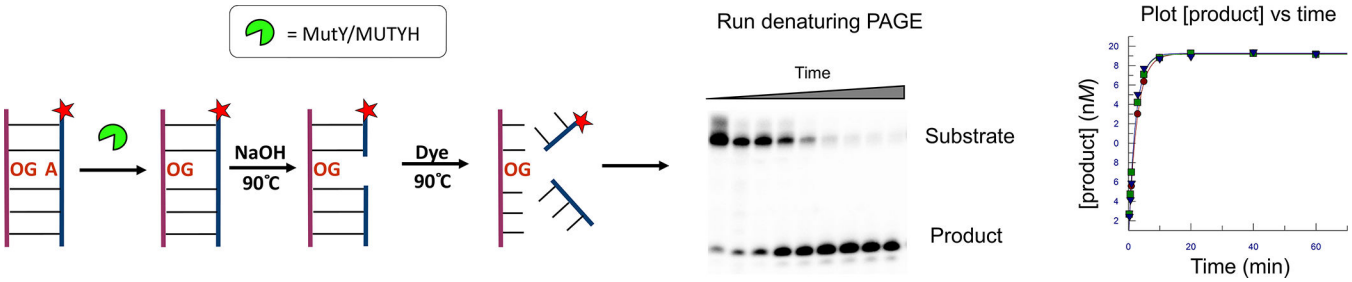

Figure 4. MutY Glycosylase Assays.

Schematic depiction of the glycosylase assay and PAGE for determination of kinetic parameters and active fractions of MutY/MUTYH.

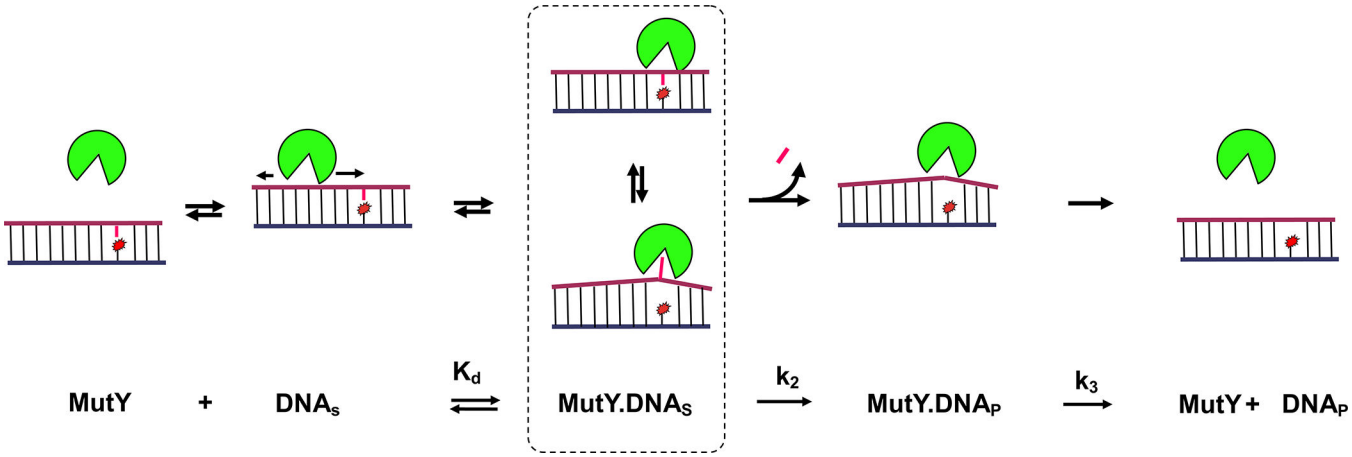

Figure 5. Schematic representation of damage processing and minimal kinetics scheme for MutY and homologs.

The free enzyme is known to non-specifically engage with the DNA strand, and use a processive search to detect the OG:A lesion. Upon encountering the lesion, it flips the adenine into its active site pocket. The binding affinity of the enzyme-substrate complex is determined by the dissociation constant K_d. The enzyme then catalyzes base excision (measured by the rate constant k_2) to form an abasic site product, which it then slowly releases (measured by rate constant k_3).

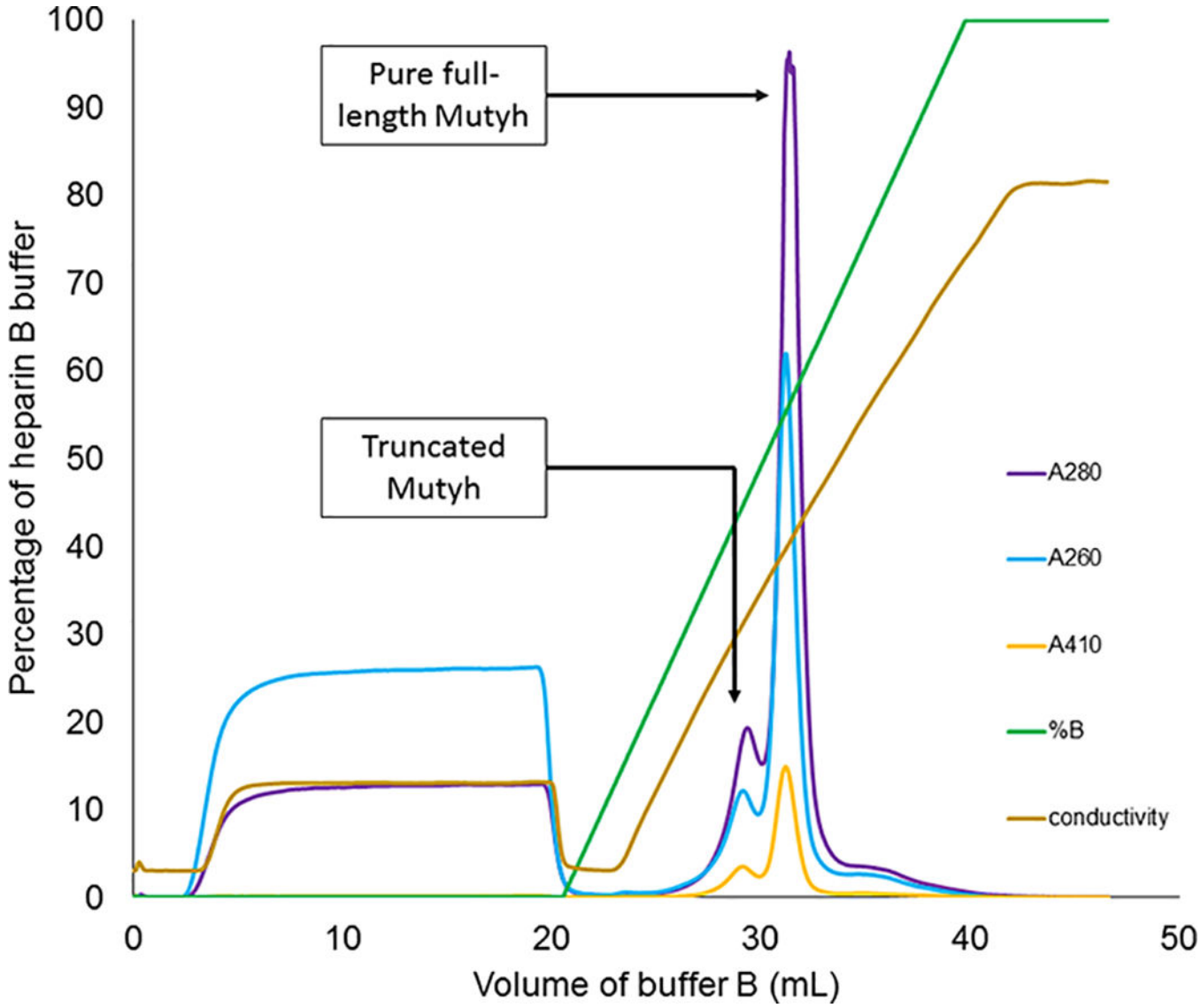

Figure 6. General Set-up for glycosylase assays

a) Set-up for a multiple-turnover/active site titration experiment showing composition of the reaction and quench tubes. **b)** Representative gel from a typical active site experiment. **c)** Characteristic plot of the concentration of product produced over time. Note, single-turnover experiments would be performed similarly by adjusting the enzyme concentration to be in excess.

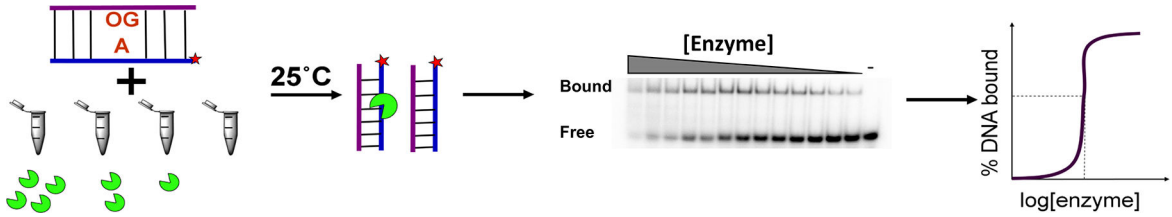

Figure 7. EMSA for determination of K_d.

Schematic illustration of assay set up, representative gel image, and expected plot of gel quantitation of K_d curve.

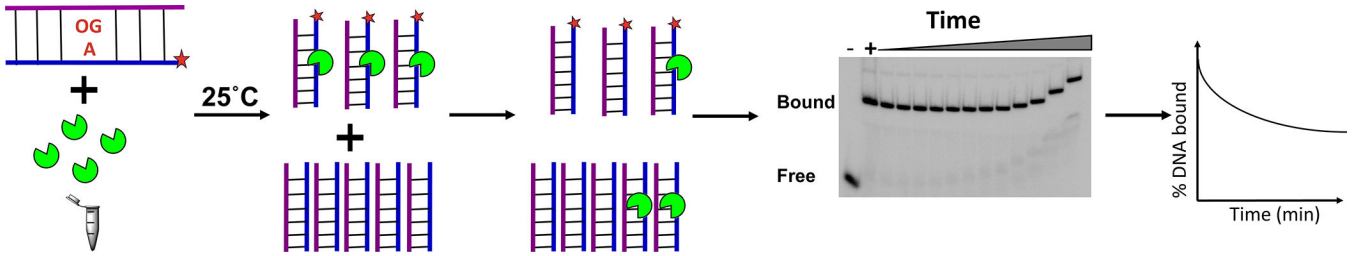

Figure 8. EMSA Determination of k_{off}.

Schematic of assay set up, representative gel of separation of enzyme bound and unbound DNA, and graphing of the image results. The first lane in gel is the negative control, containing no enzyme, second lane is positive control with no unlabeled DNA added.

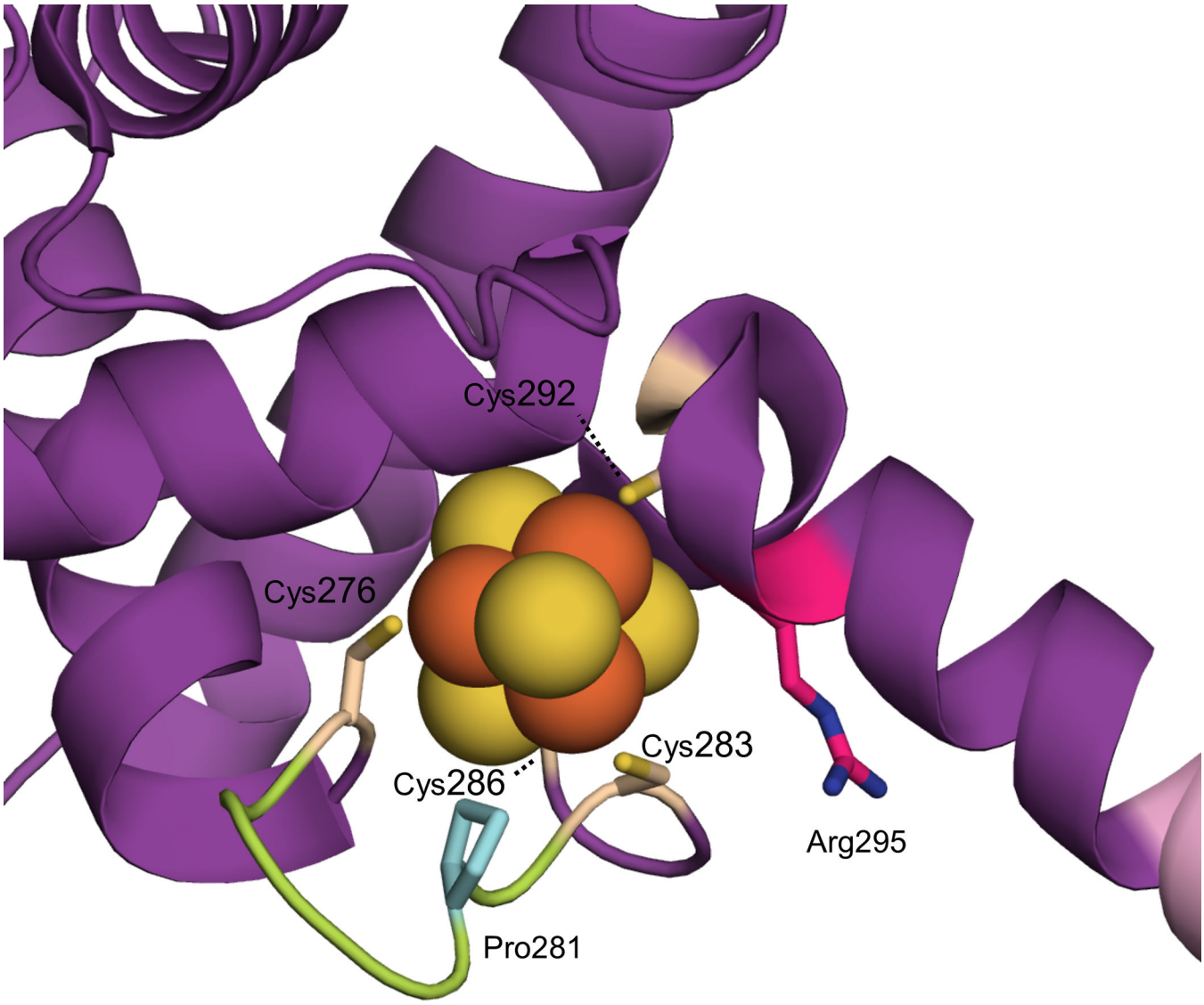

Figure 9. MAP variants located at Pro281 (cyan) and Arg295 (magenta) are adjacent the Fe-S cluster.

The MUTYH N-terminal (purple) fragment crystal structure of *Hs* MUTYH (PDB 3N5N) (Luncsford et al., 2010) contains the FCL (light green), IDC (light pink) and Fe-S cluster (orange and yellow spheres) that is coordinated by four cysteine residues (beige colored sticks)

Table 1

Summary of components and reagents necessary for the overexpression of MutY and homologs.

Enzyme Homolog	Expression Vector	Expression Host	Agar Growth Media	Culture Growth Media	Induction Conditions	Resuspension Buffer
***Ec* MutY**	pKK223-3 (no tag)	JM101 *muty*$^{-}$ cells	LB media 15 μg/ml tetracycline 100 μg/ml ampicillin 50 m*M* agar	LB media 15 μg/ml tetracycline 100 μg/ml ampicillin	1 m*M* IPTG 30 °C for 3 h 150 rpm OD600nm= 0.9	50 m*M* Tris-HCl pH 7.5 2 m*M* EDTA 5 m*M* DTT 250 m*M* NaCl Protease Inhibitor 5% glycerol
***Gs* MutY**	*pET28* (cleavable 6XHIS tag)	BL21 DE3 Rosetta 2 cells coexpressing *pRKISC*	LB media 15 μg/ml tetracycline 34 μg/ml kanamycin 50 m*M* agar	LB media 15 μg/ml tetracycline 34 μg/ml kanamycin	1 m*M* IPTG 30 °C for 6 h 150 rpm 1 m*M* $FeCl_2$ OD600nm= 0.6	20 m*M* Tris HCl pH 8.0 300 m*M* NaCl 20 m*M* imidazole 5 m*M* β-ME Protease Inhibitor
MBP Tagged *Ec* MutY	*pMAL-c2x* (MBP tag)	BL21 DE3 cells coexpressing *pRKISC*	LB media 15 μg/ml tetracycline 100 μg/ml ampicillin 50 m*M* agar	LB media 15 μg/ml tetracycline 100 μg/ml ampicillin 10 m*M* glucose	1 m*M* IPTG 30 °C for 4 h 150 rpm 1 m*M* $FeCl_2$ OD600nm= 0.5	20 m*M* sod phos. pH 7.5 1 m*M* EDTA 1 m*M* DTT 200 m*M* NaCl 1m*M* PMSF 10 % glycerol
Mouse Mutyh	*pET28* (cleavable 6XHIS tag)	BL21 DE3 cells coexpressing *pRKISC*	LB media 15 μg/ml tetracycline 34 μg/ml kanamycin 50 m*M* agar	LB media 15 μg/ml tetracycline 34 μg/ml kanamycin	1 m*M* IPTG 30 °C for 6 h 150 rpm 1 m*M* $FeCl_2$ OD600nm= 0.8	20 m*M* sod. phos. pH 7.5 1 m*M* PMSF 10% glycerol
MBP Tagged Human MUTYH	*pFastBacDual* (MBP tag)	Sf9 insect cells Baculovirus	N/A	Hyclone SfX media 25 μg/ml gentamycin	N/A	20 m*M* Tris-HCl pH 7.5 1 m*M* EDTA 1 m*M* DTT 200 m*M* NaCl Protease Inhibitor

Table 2

Summary of components and reagents necessary for the purification of MutY and homologs.

Enzyme Homolog	Tag	Separation Method	Separation Buffer A	Separation Buffer B	Heparin Buffer A	Heparin Buffer B	Storage Buffer Before Freezing
***Ec* MutY**	N/A	Salt precipitation	40% (w/v) of ammonium sulfate	N/A	20 m*M* sod. phos. pH 7.5 1 m*M* EDTA 1 m*M* DTT 5% glycerol filter/degas	20 m*M* sod. phos. pH 7.5 1 m*M* EDTA 1 m*M* DTT 5% glycerol 1 *M* NaCl filter/degas	20 m*M* sod. phos. pH 7.5 1 m*M* EDTA 1 m*M* DTT 100 m*M* NaCl
***Gs* MutY**	6X His	Ni^{2+}-NTA column	20 m*M* Tris-HClpH 8.0 300 m*M* NaCl 20 m*M* imidazole 5 m*M* *β*-ME	20 m*M* Tris-HCl pH 8.0 300 m*M* NaCl 250 m*M* imidazole 5 m*M* *β*-ME	N/A	N/A	20 m*M* Tris-HCl pH 8.0 150 m*M* NaCl 5 m*M* *β*-ME
***Ec* MutY**	MBP	Amylose column	20 m*M* sod. phos. pH 7.5 1 m*M* EDTA 1 m*M* DTT 5% glycerol 200 m*M* NaCl	20 m*M* sod. phos. pH 7.5 1 m*M* EDTA 1 m*M* DTT 5% glycerol 200 m*M* NaCl 10 m*M* maltose	20 m*M* sod. phos. pH 7.5 1 m*M* EDTA 1 m*M* DTT 5% glycerol filter/degas	20 m*M* sod. phos. pH 7.5 1 m*M* EDTA 1 m*M* DTT 5% glycerol 1 *M* NaCl filter/degas	20 m*M* sod. phos. pH 7.5 1 m*M* EDTA 1 m*M* DTT 200 m*M* NaCl
Mutyh	6X His	Ni^{2+}-NTA column	20 m*M* sod. phos. pH 7.5 10% glycerol 1 *M* NaCl 20 m*M* imidazole	20 m*M* sod. phos. pH 7.5 10% glycerol 300 m*M* NaCl 500 m*M* imidazole	20 m*M* sod. phos. pH 7.5 1 m*M* EDTA 5% glycerol filter/degas	20 m*M* sod. phos. pH 7.5 1 m*M* EDTA 5% glycerol 1 *M* NaCl filter/degas	20 m*M* sod. phos. pH 7.5 1 m*M* EDTA 200 m*M* NaCl
MUTYH	MBP	Amylose column	20 m*M* Tris-HCl pH 7.5 200 m*M* NaCl 1 m*M* EDTA 1 m*M* DTT Protease Inhibitor	20 m*M* Tris-HCl pH 7.5 200 m*M* NaCl 1 m*M* EDTA 1 m*M* DTT Protease Inhibitor 10 m*M* maltose	N/A	N/A	20 m*M* Tris-HCl pH 7.5 200 m*M* NaCl 1 m*M* EDTA 1 m*M* DTT

Table 3

Summary of equipment needed for the over expression and purification of MutY homologs and variants.

Equipment	Notable Specifications
Pipette tips/microcentrifuge tubes/conical tubes	DNase/RNase/Pyrogen free and sterile
Vortex/mini centrifuge	Table top
Thermocycler	Applied Biosystems GeneAmp PCR System 2400
Syringe filters	0.2 μm, 1 μm and 0.45 μm sterile
Gravity flow column	PD10 columns with 1 μm filter disc
Incubator/shaker	Temperature/speed control
Stir/hot plate	Temperature control
Centrifuge	Sorvall Ultracentrifuge
Sonifier	Branson sonifier 250 at 70% power
FPLC	AKTApurifier FPLC system
Concentrator	Amicon ultrafiltration cell/spin filter, 10K MWCO
0.2 μm spin filter	Corning Costar Spin-X
UV/vis	HP 8453 with OLISWorks
Western blot/SDS gel equipment	Bio-Rad
Agarose gel equipment	Bio-rad mini sub gel gt
Cold room	Maintained at 4 °C

Table 4

Composition of Solutions for Characterization Assays

Assay	2X Annealing Buffer	Gel Composition	Acrylamide: Bis acryalamide	10X Assay Buffer	MutY/MUTYH Dilution Buffer	Reaction Mix Composition
Glycosylase	40 m*M* TrisHCl pH 7.6 20 m*M* EDTA 300 m*M* NaCl	15% acrylamide 7 *M* urea 1X TBE buffer	40% 19:1	200 m*M* Tris- HCl pH 7.6 100 m*M* EDTA	20 m*M* Tris- HCl pH 7.6 10 m*M* EDTA 20% glycerol	1X assay buffer 20 n*M* DNA* 30 m*M* NaCl 0.1 mg/ml BSA
EMSA	40 n*M* TrisHCl- pH 7.6 20 m*M* EDTA 300 m*M* NaCl	6% acrylamide 0.5X TBE buffer	40% 29:1	200 m*M* Tris- HCl pH 7.6 10 m*M* EDTA 1.0 *M* NaCl	20 m*M* Tris- HCl pH 7.6 10 m*M* EDTA 20% glycerol	2X assay buffer 10 p*M* DNA* 0.2 mg/ml BSA 2 m*M* DTT 20% glycerol

DNA* refers to the radiolabeled DNA which is 5% labeled in the glycosylase assay and 100% labeled in EMSA.

Table 5

Summary of equipment needed for the glycosylase assay in order to determine the percent active fraction and intrinsic rate of glycosidic bond cleavage of MutY homologs and variants

Equipment	Notable Specifications
Pipettes/tips/microcentrifuge tubes/conical tubes	DNase/RNase/Pyrogen free and sterile
HPLC	Shimadzu prominence LC-2AT
Speed-vac centrifuge	Savant speed vac SC110
Rapid Quench Flow Instrument	Kintek Rapid Quench Flow (RQF-3)
Timer	Recording time points throughout reaction
Vortex/mini centrifuge	Table top
Ice bucket	Experiment carried out on ice
UV/vis	HP 8453 with OLISWorks
Glass plates, spacers and comb	0.35 mm thick spacers and a 32 well comb
Dry bath incubator	Fits 1.6 ml microcentrifuge tubes, temperature controlled
Phosphoimager screen	Molecular Dynamics phosphor imager screen
Phosphoimager	Typhoon 9400 scanner, GE Healthcare
Software	ImageQuaNT V.5.2. and GraFit V 5.0.2

Table 6

Summary of the equipment needed for an EMSA in order to determine the affinity of MutY homologs and variants to DNA.

Equipment	Any Notable Specifications
Pipette tips/microcentrifuge tubes/conical tubes	DNase/RNase/Pyrogen free and sterile
HPLC	Shimadzu prominence LC-2AT
Speed-vac centrifuge	Savant speed vac SC110
Timer	Recording time points throughout reaction
Vortex/mini centrifuge	Table top
Ice bucket	Experiment carried out on ice
UV/vis	HP 8453 with OLISWorks
Glass plates, spacers and comb	3 mm thick spacers and a 14 well comb
Dry bath incubator	Fits 1.6 ml microcentrifuge tubes, temperature controlled
Gel dryer	Bio-Rad Model 583 Gel Dryer
Phosphoimager screen	Molecular Dynamics phosphor imager screen
Phosphoimager	Typhoon 9400 scanner, GE Healthcare
Software	ImageQuaNT V.5.2. and GraFit V 5.0.2

Table 7

Kinetics and Binding Data for Pro281Leu, Arg295Cys and WT MUTYH

	% Active Fraction[a]	k_2 (min^{-1})[b]	K_d (n*M*)[c]
WT	100	0.90 ± 0.02	1.9 ± 0.6
Arg295Cys	5	0.4 ± 0.1	>9
Pro281Leu	0.1	No cleavage	Not bound

[a] Representative data showing the percent active fraction of (Brinkmeyer and David, 2015).

[b] The intrinsic rate (k_2) of glycosidic bond cleavage determined using the glycosylase assay under STO conditions and 150 m*M* NaCl.

[c] The equilibrium dissociation constant, K_d, as determined by EMSA of the enzyme bound to a DNA duplex with central OG:FA base pair in the presence of 100 m*M* NaCl.